NAVAL POSTGRADUATE SCHOOL
Monterey, California

THESIS

OBSERVATIONS OF MESOSCALE CONVECTIVE SYSTEMS DURING TROPICAL CYCLONE GENESIS

by
Christopher A. Finta

March, 1997

Thesis Co-Advisors: Russell L. Elsberry
Patrick A. Harr

Approved for public release; distribution is unlimited.

REPORT DOCUMENTATION PAGE

Form Approved OMB No. 0704-0188

1. AGENCY USE ONLY *(Leave blank)*	2. REPORT DATE	3. REPORT TYPE AND DATES COVERED
	March 1997	Master's Thesis

4. TITLE AND SUBTITLE
OBSERVATIONS OF MESOSCALE CONVECTIVE SYSTEMS DURING TROPICAL CYCLONE GENESIS

5. FUNDING NUMBERS

6. AUTHOR(S)
Finta, Christopher A.

7. PERFORMING ORGANIZATION NAME(S) AND ADDRESS(ES)
Naval Postgraduate School
Monterey, CA 93943-5000

8. PERFORMING ORGANIZATION REPORT NUMBER

9. SPONSORING / MONITORING AGENCY NAME(S) AND ADDRESS(ES)

10. SPONSORING / MONITORING AGENCY REPORT NUMBER

11. SUPPLEMENTARY NOTES
The views expressed in this thesis are those of the author and do not reflect the official policy or position of the Department of Defense or the U.S. Government.

12a. DISTRIBUTION / AVAILABILITY STATEMENT
Approved for public release; distribution unlimited.

12b. DISTRIBUTION CODE

13. ABSTRACT *(maximum 200 words)*

A better understanding of the role mesoscale convective systems (MCS) play in the formation stages of tropical cyclones will increase the ability to predict their occurrence and motion. This thesis employs high-resolution satellite imagery to observe the interaction between MCSs and their environment. Specifically, thirteen cases of tropical disturbances that eventually developed into tropical cyclones are analyzed to determine the role of MCSs in increasing the system organization. Following two conceptual models developed during the Tropical Cyclone Motion (TCM-93) mini-field experiment, each tropical cyclone is classified according to the relative importance of MCS activity to its development. Both conceptual models are verified through analysis and a third model is created to account for tropical cyclone developments that share features of the previous two models. An alternate approach is proposed for determining tropical system organization using only visible and infrared satellite imagery.

14. SUBJECT TERMS
Mesoscale Convective Systems, Tropical Cyclone Genesis, Formation

15. NUMBER OF PAGES
91

16. PRICE CODE

17. SECURITY CLASSIFICATION OF REPORT	18. SECURITY CLASSIFICATION OF THIS PAGE	19. SECURITY CLASSIFI- CATION OF ABSTRACT	20. LIMITATION OF ABSTRACT
Unclassified	Unclassified	Unclassified	UL

NSN 7540-01-280-5500

StandardForm298 (Rev. 2-89)
Prescribed by ANSI Std. 239-18

Approved for public release; distribution is unlimited

OBSERVATIONS OF MESOSCALE CONVECTIVE SYSTEMS DURING TROPICAL CYCLONE GENESIS

Christopher A. Finta
Captain, United States Air Force
B.S., Creighton University, 1991

Submitted in partial fulfillment of the
requirements for the degree of

MASTER OF SCIENCE IN METEOROLOGY

from the

NAVAL POSTGRADUATE SCHOOL
March 1997

Author: _____
Christopher A. Finta

Approved by: _____
Russell L. Elsberry, Thesis Co-advisor

_____
Patrick A. Harr, Co-advisor

_____
Carlyle H. Wash, Chairman
Department of Meteorology

ABSTRACT

A better understanding of the role mesoscale convective systems (MCS) play in the formation stages of tropical cyclones will increase the ability to predict their occurrence and motion. This thesis employs high-resolution geostationary satellite imagery to observe the interaction between MCSs and their environment. Specifically, thirteen cases of tropical disturbances that eventually developed into tropical cyclones are analyzed to determine the role of MCSs in increasing the system organization. Following two conceptual models developed during the Tropical Cyclone Motion (TCM-93) mini-field experiment, each tropical cyclone is classified according to the relative importance of MCS activity to its development. Both conceptual models are verified through analysis and a third model is created to account for tropical cyclone developments that share features of the previous two models. An alternate approach is proposed for determining tropical system organization through severe tropical cyclone strength using only visible and infrared satellite imagery.

TABLE OF CONTENTS

ACKNOWLEDGMENTS

I would like to thank Dr. Russell L. Elsberry for his guidance and support throughout the preparation of this thesis. He provided insight into the complex structure and processes that lead to tropical cyclones, and encouraged me to develop a conceptual framework from analyzing the data instead of vice versa. I would like to thank Dr. Pat Harr for providing the database and computer expertise that made this thesis possible. I would also like to thank Dr. Elizabeth Ritchie for her insight and suggestions which resulted in an improved alternate approach. Additionally, the efforts of the Joint Typhoon Warning Center satellite analysts in archiving the GMS satellite imagery was essential and is appreciated. Most importantly, I would like to thank my wife Flordeliza for her love, understanding and support throughout my time at the Naval Postgraduate School.

I. INTRODUCTION

Globally, an average of 80 tropical cyclones (TCs) form over the tropical oceans each year, of which nearly two thirds reach severe tropical cyclone strength (McBride 1995). The death toll and property damage inflicted by their strong winds, torrential rains, and storm surges is unparalleled by any other natural disaster (Chen 1995). Typhoons in the western North Pacific from the International Date Line to the Indian Ocean present a serious and continuing threat to United States military installations and fleet assets. A better understanding of tropical cyclone formation, structure, and motion reduces this threat by providing military decision makers with advance warning of their existence, and more accurate forecasts of their future movement, development and strength. This thesis will describe mesoscale factors that contribute to tropical cyclone formation in a pre-existing favorable synoptic environment.

A. ENVIRONMENTAL CONDITIONS FOR TC FORMATION

For the purposes of this thesis, tropical cyclogenesis or tropical cyclone formation is defined to be the process of increasing the dynamic organization of a tropical disturbance from inception until it becomes a tropical depression with a closed circulation. The favorable dynamic and thermodynamic environmental conditions necessary for tropical cyclone formation are well understood and documented. Six seasonally averaged climatological parameters that describe the slowly changing thermodynamic and rapidly changing dynamic potential of a formation region have been presented by Gray (1975, 1979). These include ocean thermal energy, surface to 500mb equivalent potential temperature differences, mid-tropospheric relative humidity, Coriolis

parameter, the inverse of the tropospheric vertical wind shear, and low-level relative vorticity. When these parameters are averaged over a statistically significant time period, they provide an excellent estimate of the long-term frequency of occurrence of tropical cyclones at nearly all global locations for each season of the year (Gray 1975). Because the first three (thermodynamic) parameters can be continuously favorable over much of the tropical ocean area and vary slowly with season, they are of little use in determining the shorter time scale events that separate developing tropical disturbances from non-developers.

It is still unclear exactly what physical differences separate tropical disturbances that develop into tropical cyclones from those likely candidates that fail to develop in a favorable climatological and synoptic environment. Erickson (1977) concluded that there are no apparent differences in the overall amount and intensity of convective cloudiness between the two. The problem is further compounded because no general agreement exists on a specific definition of tropical cyclogenesis (Lander and Guard 1995). The historical observational database in the western North Pacific region has only been adequate to represent the tropical environment on synoptic spatial and temporal scales. Until recently, high resolution geostationary meteorological satellite imagery for the western North Pacific region has been unavailable to most researchers. This lack of reliable observational data in the immediate vicinity of western North Pacific tropical disturbances prevents a complete understanding of the mesoscale dynamic processes involved in tropical cyclone genesis.

Riehl (1954) stated, "We observe universally that tropical storms form only within pre-existing disturbances ... A weak circulation, low pressure, and a deep moist

present from the beginning." From this starting point, numerous theories have been proposed on how tropical cyclone formation and development occurs. These theories involve an assumption that the processes that lead to tropical cyclone formation are different from those responsible for its further intensification. However, no primary mechanism has been isolated as being responsible for the formation of tropical cyclones (McBride 1995). One similarity in the theories is an attempt to clarify the linear and nonlinear physical processes that link the sub-synoptic features of a developing tropical disturbance to the large-scale environmental circulation. An operationally useful theory must describe the mesoscale dynamic processes occurring within tropical disturbances and how they interact with the larger scale environmental conditions. An important aspect of this interaction is delineating the moment when a tropical cloud cluster changes from an unorganized system to an organized tropical disturbance, and the exact physical processes that caused the change.

B. ROLE OF MESOSCALE FEATURES IN TC FORMATION

Zehr (1992) has proposed a two-stage formation model in which mesoscale convection plays a critical role as the catalyst that organizes a cloud cluster into a tropical depression. Stage one consists of the onset of a large area of vigorous convection (associated with the early convective maximum) followed by the dissipation of this mesoscale convective system (MCS). At this time, a distinct low-level circulation center (LLCC) can first be identified on satellite imagery as a persistent series of cyclonically curved cumulus lines spiraling into the LLCC. A highly variable time period of between twelve hours to several days may elapse until the next stage begins. Stage two is marked by the onset of increasing deep convective activity associated with the low-level

circulation center. It is usually at this time that the tropical disturbance is first designated a tropical depression. One other feature of this model is the speculation that the convective activity in both stages is the result of a wind surge that penetrates into the center of the cloud cluster and enhances the low-level confluence (Zehr 1992). This hypothesis, based on three-hourly, 10-km resolution visual and infrared satellite imagery, will be discussed in more detail later.

It is also hypothesized that the structure of MCSs during tropical cyclone formation may determine future aspects of the tropical storm, such as size (and therefore the deflection of its motion from environmental steering) and intensity. Therefore, the role of MCSs in tropical cyclogenesis becomes especially important and has been studied extensively in recent years (Elsberry et al. 1995). A tropical MCS has many of the characteristics of a midlatitude Mesoscale Convective Complex (MCC) such as life cycle, duration, and size distribution (Ibid). A MCS is defined here as a convective system of one or more thunderstorms with cloud-top temperatures with an areal extent of the 209°K isotherm over a minimum of 10,000 square kilometers and a duration of at least 6 hours. A tropical cloud cluster may contain zero, one, or more MCSs at a particular time.

It has been proposed that a cloud cluster can make the transition from unorganized system to organized tropical depression in less than one day in association with a MCS (Chen and Frank 1993). The concentrated vertical ascent and latent heat release in the stratiform region of a MCS contributes to formation of a Mesoscale Convective Vortex (MCV) in the middle troposphere. According to this theory, a local reduction of the vertical stability and in the Rossby radius of deformation also results. Because latent heat release is more efficient in increasing the temperature perturbation and the rotational

winds in a saturated environment, the spinup time for the cloud cluster may be reduced from days to only 12 hours, which is the time scale of a diurnal cycle of deep convection (Ibid). The mechanism by which the MCV translates downward and taps into the heat and moisture sources of the planetary boundary layer remains unknown. This process has been numerically modeled for mid-latitude squall lines by Hertenstein and Schubert (1991), who indicate that the stratiform region may be associated with a large positive mid-tropospheric potential vorticity anomaly. Translation of a land-based MCV over a warm ocean has been observed to result in the development of a tropical cyclone (Velasco and Fritsch 1987).

C. CONCEPTUAL MODELS OF TC FORMATION DURING TCM-93

The formation stages of several tropical cyclones were observed during the Tropical Cyclone Motion 93 (TCM-93) mini-field experiment in the western North Pacific during July and August 1993 (Harr et al. 1996a, b). Aircraft, satellite, station, rawinsondes, and omega dropwindsonde (ODW) observations were used to analyze MCS and MCV structures in the region of developing tropical cyclones. A two-dimensional, multiquadric interpolation technique (Nuss and Titley 1994) was used to analyze the data within the dense aircraft observation region. Two separate genesis pathways were hypothesized to account for the significant differences in the synoptic and mesoscale processes that contributed to the formation of one midget (Harr et al. 1996a) and one large tropical cyclone (Harr et al. 1996b).

Two aircraft observing periods (AOP-1A and AOP-1B) early in the course of TCM-93 covered the formation stages of the midget tropical cyclone Ofelia. During these flights, three distinct mesoscale convective vortices were located by aircraft and

ODW observations in areas of persistent deep convection. The first two MCVs were well defined at 500 mb, but were located above areas of strong, straight southwesterly low-level wind flow. Thus, they quickly dissipated because they were unable to propagate downwards and tap into the energy of the planetary boundary layer (PBL). However, the third MCV was located above an area of low-level cyclonic shear and its structure extended down to at least 850 mb. It is believed that because of the greater vertical extent and location on the cyclonic shear side of the large-scale flow, the third MCV was able to extend vertically into the PBL and exploit the thermodynamic energy resources of that layer to further increase its organization. High-resolution geostationary satellite imagery was used by Harr et al. (1996a) to document the explosive convective development associated with this low-level circulation center that led to the formation of Tropical Storm Ofelia. In this instance, the primary pathway towards tropical cyclone formation is hypothesized to have been an increase in low-level cyclonic vorticity and lowering of the surface pressure caused by mesoscale convective systems located in a favorable synoptic environment.

More than ten days after the formation of TS Ofelia, a large monsoon depression that defined a region of low pressure, cyclonic winds, and convective activity moved westward into the monsoon trough that was extending through the Philippine Sea. The overall circulation observed during AOP-3A was very broad with a line of confluence on its southeastern side and a dissipating MCS on the eastern periphery that represented a maximum of potential vorticity. The 850 mb and 700 mb circulation of the monsoon depression shifted towards the location of the MCS, while the 500 mb circulation center was located over the low-level center of the overall broad circulation. Following the

dissipation of this MCS, new MCSs developed to its north and south. The southern MCS dissipated and convection to the south of the monsoon depression center became aligned in bands that may have separated and protected the developing tropical cyclone from external effects that might have proved detrimental to system development. Although lower- and upper-level momentum sources contributed to the monsoon depression circulation, transformation to a tropical cyclone did not occur until the northern MCS became the monsoon depression center. The increase of cyclonic winds in the area of the monsoon depression was accompanied by an import of cyclonic angular momentum at low levels needed to increase the organization of the system towards tropical cyclone genesis. Based on the analyses from the second flight (AOP-3B), the primary pathway to tropical cyclone formation is hypothesized to have been the increase in low-level relative vorticity provided by the synoptic environment.

D. OBJECTIVES OF THIS THESIS

Given these two tropical cyclogenesis pathways identified during TCM-93, this thesis employs high spatial and temporal resolution Geostationary Meteorological Satellite (GMS) imagery and global model analyses to examine the interaction between mesoscale features and the large-scale environment during other cases of tropical cyclogenesis. The initial conceptual models are based on the TS Ofelia (Harr et al. 1996a) and Typhoon (TY) Robyn (Harr et al. 1996b) TCM-93 data sets. Just as in the two-stage model (Zehr 1992), the TC formation may involve a (or several) MCS.

The first of these potential pathways for tropical cyclogenesis is characterized to be more strongly dependent on the activity of the mesoscale components. The second pathway is characterized to be influenced more by the large-scale environmental winds

with the mesoscale component being less important until the final focusing of the circulation about the center. A key objective of this thesis is to verify or modify these conceptual models on a larger sample of TC formations based primarily on the higher space and time resolution satellite imagery without the benefit of aircraft observations. A total of 13 developing tropical cyclones are tracked backward in time from when they became named tropical storms until no identifiable features could be analyzed. The objective is to classify the satellite-observed features of the cloud cluster development into one of the two original conceptual models, if possible. In non-conforming cases, analysis of the high spatial and temporal resolution satellite image loops is used to propose modifications to the conceptual models to account for additional features that have been found to be important. In some cases, both the mesoscale and synoptic-scale processes seem to be contributing simultaneously to the TC formation.

II. METHODOLOGY

A. DATA

The key data for this thesis are the high temporal and spatial resolution imagery from the Japanese Geostationary Meteorological Satellite (GMS-4 and GMS-5). To observe the relatively short time scale of MCS development and dissipation, hourly visible and infrared images were animated. Up to 30 hours of GMS high resolution imagery were animated at a time for a grid from 0° to 30° N and 120° to 170° E . Thus, no TC formations over the South China Sea are included in this data set. Analyzed systems were selected from tropical cyclones occurring in the western North Pacific from August 1994 through September 1996 (see Tables 3-1 through 3-3). Systems with extended or multiple gaps in the imagery database were excluded from the data set. The analysis period studied extended from the tropical storm stage, as defined by the Joint Typhoon Warning Center (JTWC) in their Annual Tropical Cyclone Reports (ATCR), backward in time until no identifiable features definitely associated with the tropical disturbance could be detected. To determine the synoptic-scale environment in which the systems formed, the 00 UTC and 12 UTC GMS images were digitally overlaid, whenever possible, with Naval Oceanographic Global Atmospheric Prediction System (NOGAPS) streamline fields at the 850 mb and 200 mb levels.

All software packages were run on the IRIS 5.3 UNIX system on Silicon Graphics Indigo workstations. The hourly satellite imagery was processed with the NSAT software package, with a resolution of 8 kilometers in both the visible (from 20 - 07 UTC) and in the infrared. The NSAT algorithm allowed precisely navigated latitude and longitude gridding to be overlaid on the raw imagery, as well as zooming, color enhancement of the

infrared images, and forward and backward looping. The overlays of GMS images and NOGAPS streamlines, which were created using GEMPAK 5.2.1, are available in .GIF format via the Internet at the following Universal Resource Locator: [http://www.met.nps.navy.mil/~cafinta/thesisA/table.html].

B. ANALYSIS PROCEDURES

The TC formations in the data set were to be analyzed and classified into two categories dependent upon which conceptual model developed from the two TCM-93 cases best represented the dominant contributions to tropical cyclone genesis. Those TCs that had vigorous, sustained MCS / MCV activity, and relatively weak synoptic forcing, were classified as Ofelia-type formations (Table 2-1). Those formations with strong contributions from the synoptic flow, and relatively weak or only peripheral MCS activity, were classified as Robyn-type formations (Table 2-2).

Tropical mesoscale convective systems can produce MCVs without attaining the size or duration of mid-latitude mesoscale convective complexes (Harr et al. 1996a, 1996b). Therefore, the delineation between a MCS as defined in Chapter I.B and a large thunderstorm or group of adjacent thunderstorms that did not meet minimum MCS size, intensity, and/or duration was important. The definition of a mesoscale convective system in Chapter I.B was used to separate the two categories of convective activity. From the earliest detectable time, the occurrence and characteristics of each MCS in a tropical disturbance were recorded. The following variables were initially included:

1. Rapid growth / decay of the MCS. Rapid growth means the MCS developed

		SYSTEM		*MCS*								
Cyclone	Date Time Group	Cloud system size	Principal band shielding	Rapid growth / decay	Peripheral location	Forms next to decaying MCS	Vigorous central updraft	Inner spiral bands	Cross equatorial flow reaches MCS	Has weak convective organization	Outflow aloft is radial or anti-cyclonic	Latitude of MCS (°N)
Pre-Organization	Stage											
Seth94 MCSA	2Oct/00 - 07	Medium	N	Y / Y	N	Unknown	Y	N	Y	Y	R	8
Seth94 MCS B	2Oct/16 - 22	Medium	N	Y / Y	N	Y	N	Y	Y	N	R	10
Teresa94 MCS A	15Oct/05-11	Small	N	Y / N	Y	N	N	N	N	Y	R	17
Teresa94 MCSB	15Oct/17-22	Small	N	Y / Y	N	Y	Y	Y	N	N	R	15
Faye95 MCS A	14Jul/10-15	Medium	N	Y / Y	N	Y	Y	Y	Y	Y	R	10
Faye95 MCS B	14Jul/14-19	Medium	N	Y / Y	Y	Y	N	Y	Y	Y	R	10
Zack95 MCS A	24Oct/17-20	Medium	N	Y / Y	Y	N	N	Y	Y	Y	R	12
Zack95 MCS B	24Oct/17-25/02	Medium	N	Y / N	N	N	N	Y	Y	Y	R	8
Angela95 MCS A	25Oct/04-08	Medium	N	Y / Y	Y	N	N	Y	???	Y	R	8
Yates96 MCS A	20Sep/17-22	Small	N	Y / Y	N	Unknown	N	Y	N	Y	R	11
Yates96 MCS B	21Sep/18 - 22/04	Small	N	Y / Y	N	N	N	Y	N	Y	R	13
Organization	Stage											
Seth94 MCS C	3Oct/03 - 08	Medium	N	Y / N	N	Y	Y	Y	Y	N	A	10
Seth94 MCS D	3Oct / 14 on	Medium	Y	Y / N	N	Y	Unknown	Y	Y	N	A	10
Teresa94 MCS C	16Oct/05-10	Small	N	Y / Y	N	N	Y	Y	N	Y	A	16
Teresa94 MCS D	16Oct/14 on	Small	N	Y / N	N	Y	Y	Y	N	N	R	16
Faye95 MCS C	15Jul/12 on	Medium	Y	Y / ?	N	N	Y	Y	Y	N	A	14
Zack95 MCS C	25Oct/08 on	Medium	N	N / N	N	N	Y	Y	Y	N	A	9
Angela95 MCS B	25Oct/07-19	Medium	N	Y / N	N	N	Y	Y	???	N	A	10
Angela95 MCS C	25Oct/18 on	Medium	N	Y / N	N	Y	Y	Y	???	N	A	12
Yates96 MCS C	22Sep/06 - 20	Medium	Y	Y / N	N	N	Y	Y	N	N	R	15
Yates96 MCS D	22Sep/22 on	Medium	Y	Y / N	N	Y	Y	Y	N	N	A	16

Table 2-1. Summary of Chapter II.B variables for Ofelia-type formations.

		SYSTEM		*MCS*								
Cyclone	Date Time Group	Cloud system size	Principal band shielding	Rapid growth / decay	Peripheral location	Forms next to decaying MCS	Vigorous central updraft	Inner spiral bands	Cross equatorial flow reaches MCS	Has weak convective organization	Outflow aloft is radial or anti-cyclonic	Latitude of MCS (°N)
Pre-organization	Stage											
Robyn93 MCS A			N	Y / Y	Y	N	N	N	Y	Y	R	
Robyn93 MCS B			N	Y / Y	Y	N	N	N	Y	Y	R	
Fred94 MCS A	13Aug/06 - 13	Medium	Y	Y / Y	N	N	N	???	N	Y	R	20
Zane96 MCS A	??? - 20Sep/12	Medium	N	? / N	Y	???	Y	???	Y	N	R	8
Zane96 MCS B	20Sep/10 - 17	Large	N	Y / Y	Y	N	Y	N	Y	Y	R	8
Zane96 MCS C	21Sep/13 - 18	Large	N	N / Y	Y	N	Y	N	Y	Y	R	7
Zane96 MCS D	22Sep/16 - 22	Large	N	Y / Y	N	N	Y	Y	Y	N	R	6
Zane96 MCS E	23Sep/12 - 24/04	Large	Y	N / N	N	N	Y	Y	Y	Y	A	13
Organization	Stage											
Robyn93 MCS C			Y	Y / N	N	Y	Y	Y	Y	N	A	
Fred94 MCS B	14Aug/09 on	Large	Y	N / N	N	N	Y	Y	N	N	A	17
Zane96 MCS F	24Sep/09 on	Large	Y	Y / N	N	Y	Y	Y	Y	N	A	16

Table 2-2. Summary of Chapter II.B variables for Robyn-type tropical cyclone formations.

from a small thunderstorm or group of thunderstorms to the above-defined MCS size in four hours or less. Rapid decay means that the active convection associated with a fully developed MCS collapsed in the same time span, although the complete dissipation of its cirrus shield may not have occurred. Non-rapid growth or decay implies either that the MCS is composed of multiple thunderstorms—each developing and collapsing separately over a period of time—or that the processes leading to MCS formation are stronger than normal.

2. Peripheral location of the MCS. This indicates whether the MCS was located on the periphery or was co-located with the system low-level circulation center.

3. Form next to decaying MCS. A new MCS can be generated by low-level convergence from the outflow boundary of a nearby dissipating MCS. The new MCS was determined to have formed next to a decaying MCS if it developed during, or within three hours following, the previous MCS collapse. Additionally, the new MCS must have formed within one degree of latitude of—but not directly over—the dissipating MCS.

4. Vigorous central updraft. Color infrared images were analyzed for the lowest cloud-top temperature; MCSs with temperatures less than -80°C were categorized as having a vigorous deep convection.

5. Cross-equatorial flow. The presence of cross-equatorial flow contributing low-level confluence or shear vorticity to the equatorward side of the tropical system was determined by examining the NOGAPS streamlines and observing the movement of low-level clouds in the GMS imagery.

6. Weak convective organization. A MCS categorized as having weak convective organization lacked a vigorous central updraft and had gaps in the deep

convection over its interior. For example, a MCS composed of individual, loosely connected thunderstorms was considered to have weak convective organization.

7. Cloud System Size. This subjective measurement was made at the time when the Joint Typhoon Warning Center first classified the system as a tropical storm. Using visible imagery whenever possible, the extent of cyclonically curved low-level cumulus cloud lines spiraling into the system circulation center was determined.

After a preliminary analysis and discussion of the storms in the data set, additional features were proposed as being potentially important to the tropical system organization. First, a third category (Table 2-3) was created to account for tropical cyclones whose formation appeared to be attributable to a combination of strong synoptic forcing and vigorous MCS activity. The following variables were added to the tables and previously analyzed storms were re-analyzed:

8. Inner spiral bands. A MCS was determined to have inner spiral bands if rotation of the MCS was evident, or if cyclonically curved mid- or low-level cloud lines were detected following the dissipation of the cirrus shield.

9. General radial outflow aloft. Such outflow exists when the cirrus anvil of a MCS retains a uniform, nearly circular shape, which indicates an upper-level environment of low vertical wind shear, or lack of development of an organized anticyclonic outflow aloft.

10. Principal band shielding. The development of cyclonically curved convective cloud bands around the system center, whether associated with the MCS outflow or not,

		SYSTEM		*MCS*								
Cyclone	Date Time Group	Cloud system size	Principal band shielding	Rapid growth / decay	Peripheral location	Forms next to decaying MCS	Vigorous central updraft	Inner spiral bands	Cross equatorial flow reaches MCS	Has weak convective organization	Outflow aloft is radial or anti-cyclonic	Latitude of MCS (°N)
Pre Organization	Stage											
Ellie94 MCS A	??? - 1Aug/21	Small	N	??? / Y	N	Unknown	N	Y	N	Y	A	30
Ellie94 MCS B	2Aug/03 - 07	Small	N	Y / Y	N	N	N	Y	N	Y	R	29
Ellie94 MCS C	3Aug/21 - 4/01	Medium	N	N / Y	Y	N	N	Y	N	Y	R	28
Ellie94 MCS D	4Aug/04 - 5/05	Medium	N	N / N	Y	N	N	Y	N	Y	R	27
Gladys94 MCS A	??? - 19Aug/00	Medium	N	??? / Y	N	Unknown	Unknown	Y	N	Y	A	13
Gladys94 MCS B	19Aug/16 - 20	Medium	Y	Y / Y	N	N	N	N	N	Y	R	15
Kinna94 MCS A	??? - 2Sep/22	Large	N	??? / Y	Y	Unknown	N	N	Y	Y	R	16
Kinna94 MCS B	??? - 2Sep/22	Large	N	??? / Y	N	???	Y	Y	Y	N	R	13
Kinna94 MCS C	3Sep/06 - 12	Large	N	Y / Y	N	N	N	Y	Y	Y	R	17
Kinna94 MCS D	3Sep/20 - 4//02	Large	N	N / Y	Y	Y	N	N	Y	Y	R	15
Helen95 MCS A	4Aug/18 - 5/00	Medium	N	Y / Y	N	Unknown	N	Y	N	Y	R	13
Helen95 MCS B	6Aug/17 - 23	Large	N	N / Y	Y	N	Y	Y	Y	Y	A	14
Sibyl95 MCS A	22Sep/17-23/01	Medium	N	Y / Y	N	Unknown	Y	Y	N	Y	R	6
Sibyl95 MCS B	24Sep/15-21	Medium	N	Y / Y	Y	N	Y	Y	N	N	R	3
Sibyl95 MCS C	25Sep/12-19	Large	N	Y / Y	Y	N	N	N	Y	Y	R	4
Sibyl95 MCS D	25Sep/14-26/06	Large	N	N / N	N	N	N	Y	Y	Y	R	8
Organization	Stage											
Ellie94 MCS E	5Aug/11 - 23	Medium	N	Y / Y	N	N	N	Y	N	Y	R	25
Ellie94 MCS F	6Aug/00 - 23	Large	N	Y / N	N	Y	Y	Y	N	N	A	24
Ellie94 MCS G	7Aug/11 on	Large	Y	Y / N	N	N	Y	Y	N	N	A	24
Gladys94 MCS C	20Aug/05 - 18	Medium	N	N / Y	N	N	Y	Y	Y	N	R	18
Kinna94 MCS E	4Sep/04 - 10	Large	N	Y / Y	N	N	Y	Y	Y	Y	A	19
Kinna94 MCS F	4Sep/12 - 23	Large	N	Y / N	Y	Y	Y	N	Unknown	N	R	19
Kinna94 MCS G	5Sep/02 - 06	Large	N	Y / Y	N	Y	Y	Y	Unknown	Y	A	19
Kinna94 MCS H	5Sep/06 - ON	Large	Y	Y / N	N	Y	Y	Y	Unknown	N	A	22
Helen95 MCS C	7Aug/08 - ???	Large	Y	Y / ???	Y	N	Y	???	Y	Y	R	15
Helen95 MCS D	??? - 8Aug/10	Large	N	??? / Y	N	Unknown	N	N	Y	Y	R	16
Helen95 MCS E	08Aug/09 on	Large	Y	Y / ???	N	Y	Y	Y	Y	N	R	18
Sibyl95 MCS E	26Sep/22 on	Large	N	Y / N	N	N	Y	Y	Y	N	R	9

Table 2-3. Summary of Chapter II.B variables for Combination-type tropical cyclone formations.

is taken as an indicator that the central core of the tropical system is being shielded from detrimental external processes such as vertical wind shear. Thus, a centrally located MCS that develops within a principal band would develop in a more dynamically favorable environment.

11. System dependent on MCS. The upgrading of a tropical depression to the minimum tropical storm stage requires the presence of deep convection over the system center. However, a tropical cloud cluster or tropical disturbance can be upgraded as a strong tropical depression without the presence of vigorous, centrally-located MCS activity, through synoptically-driven processes. This category represents a subjective assessment of whether or not such organization was critically dependent upon its MCSs or whether synoptic forcing was sufficient.

12. Latitude of MCS. This variable is an indicator that larger values of the Coriolis parameter are favorable for tropical cyclone development.

In summary, the classification of each tropical cyclone formation is based on animation of high-resolution satellite visible and infrared imagery. However, each case is put into the synoptic circulation context based on the NOGAPS streamline analyses. Other favorable or detrimental environmental factors are inferred from the animated imagery, such as the absence or presence of vertical wind shear impinging on the circulation. The objective of making the table entries is to summarize each stage leading up to the TC formation, and thus categorize each formation as: (i) predominately MCS-driven; (ii) predominately synoptically-driven in which MCS are present but not considered as the leading cause of formation; or (iii) both MCS and synoptic circulations must be considered as prime contributors to the formation.

III. TROPICAL FORMATIONS

A. OFELIA-TYPE

The first pathway to tropical cyclone genesis discussed in Chapter I.C involves an increase in low-level cyclonic vorticity and the lowering of the surface pressure predominately caused by mesoscale convective systems. Six of the 13 formations analyzed were classified as Ofelia-type cases. In this section, two specific examples of an Ofelia-type case will be reviewed and the trends in the variables in this data subset of TC formations will be examined.

Of the six Ofelia-type formations, Typhoon Teresa and Super Typhoon Yates provide key insights into the processes occurring in a MCS-driven tropical cyclone genesis. Typhoon Teresa developed from an easterly wave into a small tropical cyclone in the western North Pacific during mid-October 1994 (Fig. 3.A.1). The pre-Teresa tropical disturbance formed northeast of an inactive monsoon trough and by 22 UTC 14 October 1994 was located at 15°N, 152°E. At this time, scattered thunderstorms were observed in association with a weak LLCC. Although the synoptic environment was thermodynamically favorable for convection, it was weakly dynamically favorable as the system drifted west separated from cross-equatorial flow and the monsoon trough.

From 23 UTC 14 October - 04 UTC 15 October (Fig. 3.A.2), a large thunderstorm developed over the LLCC. However, it did not meet the above MCS criteria. At 05 UTC 15 October, a cluster of thunderstorms developed north and east of the LLCC (Fig. 3.A.3) and merged into a multi-celled MCS, which is identified as MCS A in Table 2-1. The collapse of MCS A from 12 -16 UTC 15 October was followed by the growth of a small MCS (labeled MCS B) directly over the LLCC at 15°N, 150°E (Fig. 3.A.4). Although

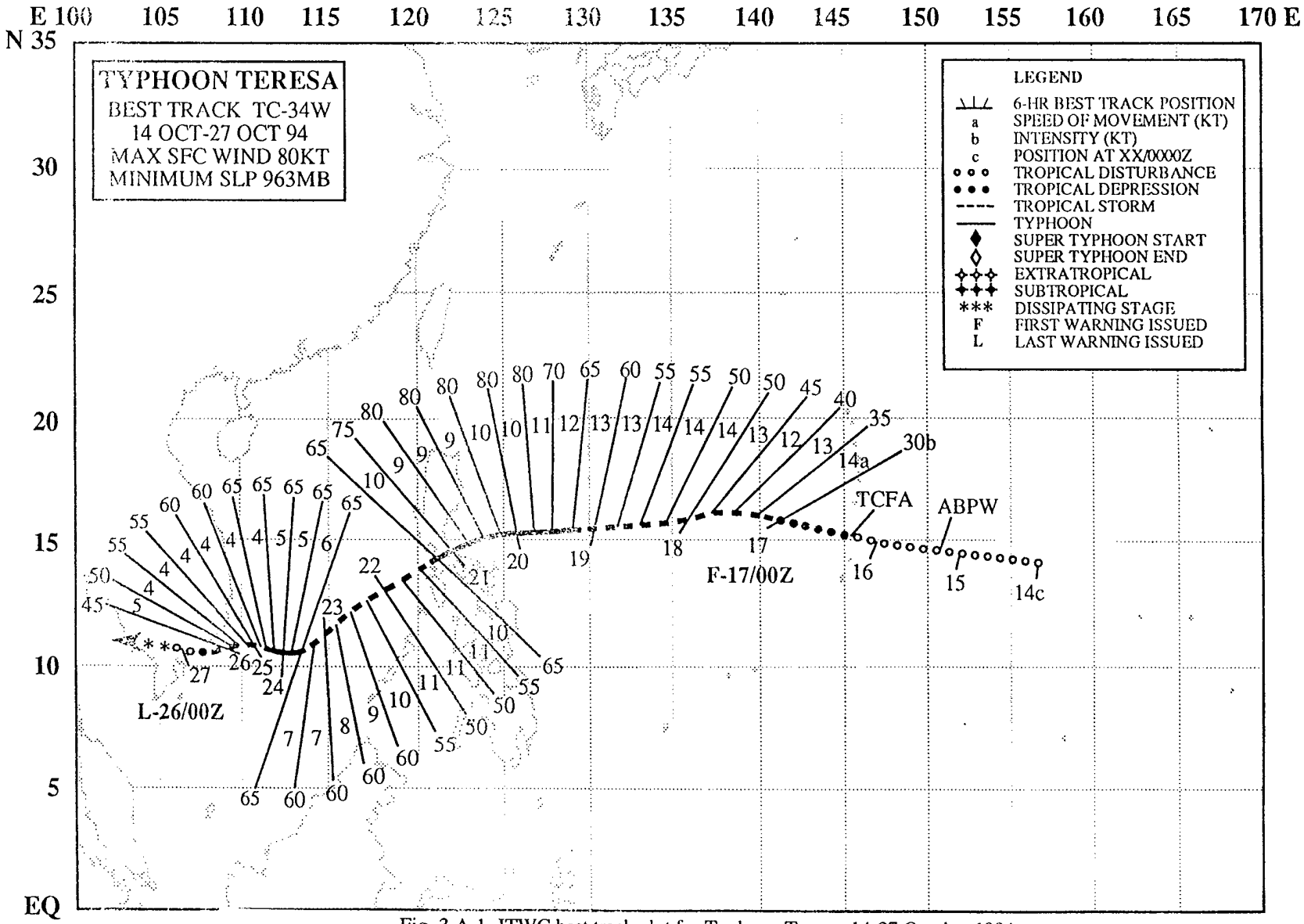

Fig. 3.A.1 JTWC best track plot for Typhoon Teresa, 14-27 October 1994.

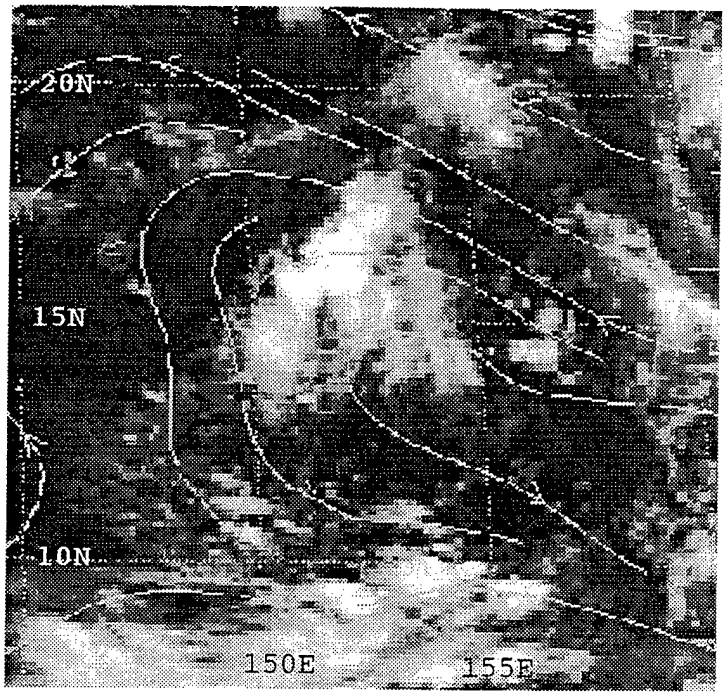

Fig. 3.A.2 Infrared GMS image and NOGAPS 850mb analyzed streamlines at 0030 UTC 15 October 1994 prior to formation of Typhoon Teresa.

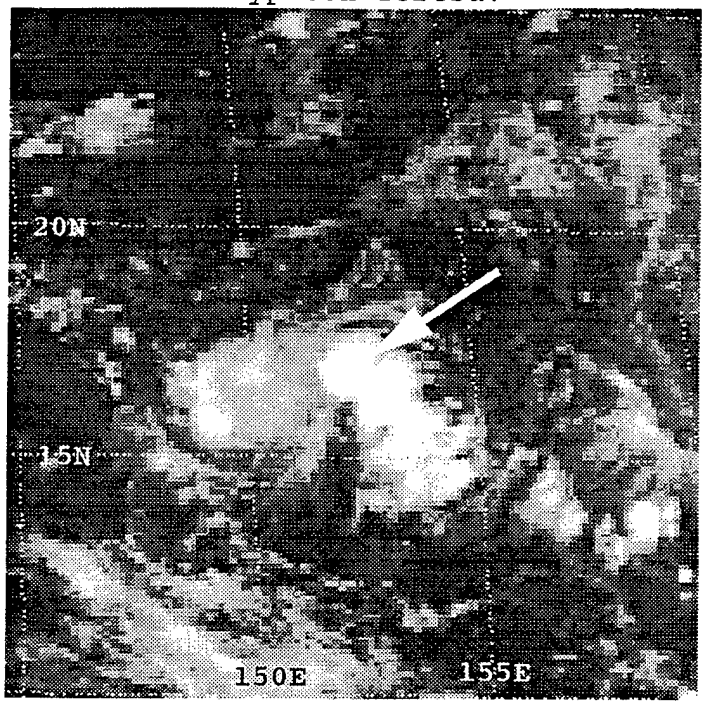

Fig. 3.A.3 As in Fig. 3.A.2, except at 05 UTC 15 October 1994 and without NOGAPS streamlines. Arrow indicates thunderstorms that form MCS A.

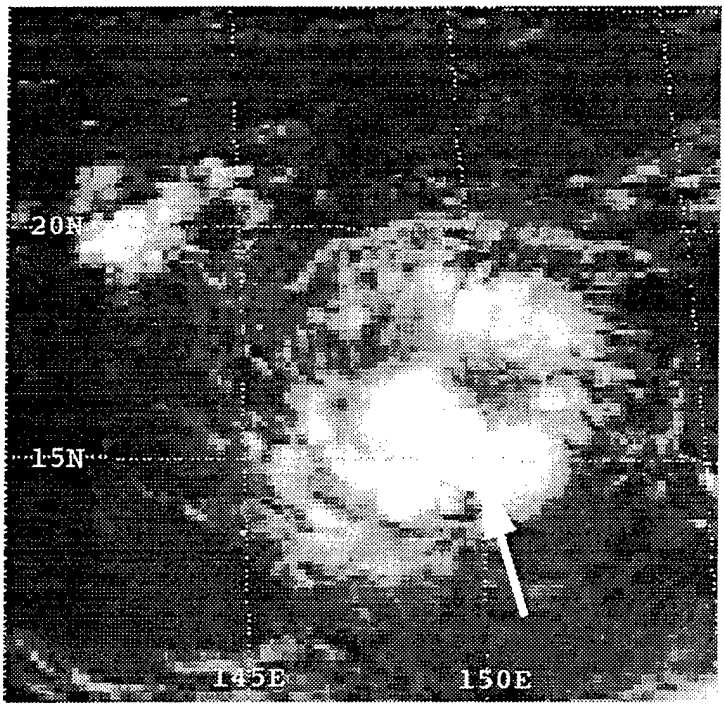

Fig. 3.A.4 As in Fig. 3.A.3, except at 17 UTC 15 October 1994. Arrow indicates MCS B.

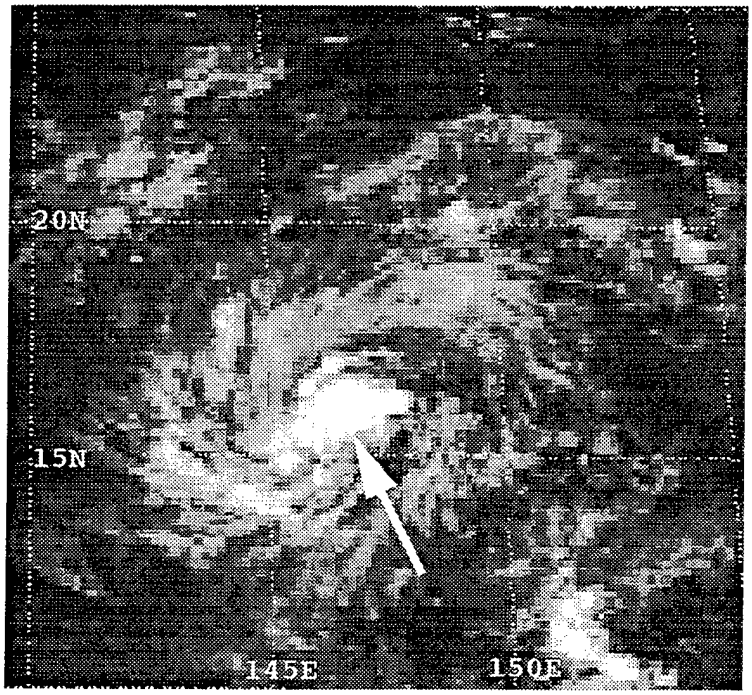

Fig. 3.A.5 As in Fig. 3.A.3, except at 05 UTC 16 October 1994. Arrow indicates MCS C.

small, the central location and greater convective organization of MCS B appeared to contribute to an increase in the strength of the LLCC. As the cirrus shield over MCS B dissipated, the LLCC cumulus lines were more cyclonically oriented, extended farther outward, and rotated faster. By 01 UTC 16 October, the upper-level cirrus outflow was clearly rotating anticyclonically. The mesoscale activity thus appeared to contribute to the spin up of the cyclonic circulation of the entire system and marked the transformation to a tropical depression.

The next cycle of deep convection began at 05 UTC 16 October as a small thunderstorm that rapidly grew into a MCS (labeled MCS C) over the LLCC. This MCS was accompanied by an arc-shaped outbreak of deep convection from the northwest to the north and northeast, and the cirrus shield expanded radially (Fig. 3.A.5). Even though MCS C collapsed at 10 UTC, it was subsequently replaced at 15 UTC by another centrally-located MCS, which is labeled MCS D in Table 2-1. Although JTWC's first warning was not issued until 00 UTC 17 October, the system could perhaps have been named a tropical storm as early as 16 UTC 16 October when the tropical system was rotating strongly with continuous deep convection at its core and with an anticyclonic outflow layer aloft.

Super Typhoon Yates provides another example of mesoscale forcing processes during tropical cyclone genesis. Super Typhoon Yates developed from an easterly wave into a small, intense tropical cyclone in the western North Pacific during late September 1996 (Fig. 3.A.6). The pre-Yates tropical disturbance formed to the northeast of a broad monsoon depression circulation and by 10 UTC 20 September 1996 was located at 11°N, 173°E. The synoptic environment in the area of the pre-Yates disturbance was

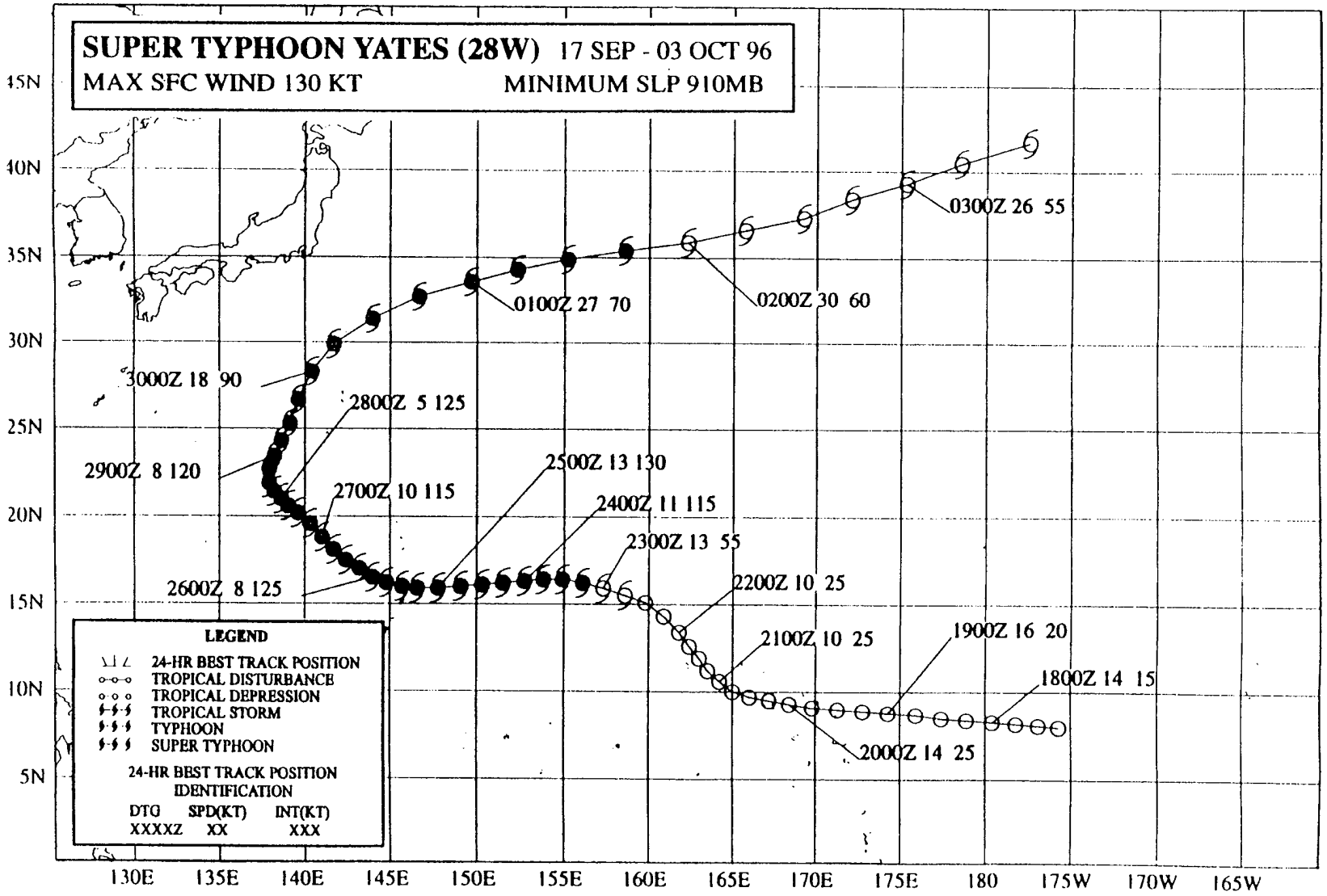

Fig. 3.A.6 As in Fig. 3.A.1, except for Super Typhoon Yates, 17 September - 3 October 1996.

thermodynamically favorable for convection and—although not connected with the active monsoon trough—was weakly dynamically favorable. Separation from the monsoon trough was a consistent feature as the system drifted towards the west-northwest.

From 17 - 22 UTC 20 September (Fig. 3.A.7), a small MCS identified as MCS A in Table 2-1 developed in the center of the pre-Yates tropical disturbance. As the MCS convection collapsed and the cirrus cover dissipated, a tightly curved series of cumulus lines was spiraling into the system circulation center. More than 48 hours prior to its classification as a minimal strength tropical storm by the JTWC, the pre-Yates tropical disturbance exhibited a high degree of dynamic organization that would persist through time. Although the system remained convectively dormant through the diurnal minimum, deep convection at 18 UTC 21 September (Fig. 3.A.8) slowly developed over more than four hours into a second centrally located MCS labeled as MCS B. Even though the convection seemed to be weakly organized, the MCS B later at 04 UTC 22 September exhibited strong rotation via well-wrapped cyclonic cumulus lines after the cirrus canopy dissipated (Fig. 3.A.9).

The third cycle of convection began only two hours later (Fig. 3.A.10) when a cluster of small thunderstorms over the LLCC explosively developed into a vigorous, long-lived and well-organized MCS labeled MCS C. Although the outflow aloft remained generally radial in shape, cyclonically curved principal bands of convection formed around the system center, which appeared to shield the inner core from adverse synoptic effects. At this time, it became obvious that the cyclonic rotation had expanded from the LLCC to involve the entire system and all of its convective elements. At 18

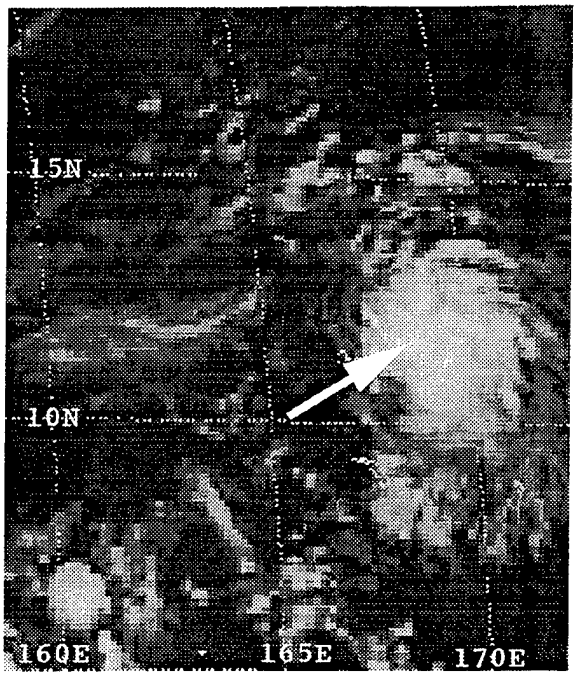

Fig. 3.A.7 As in Fig. 3.A.3, except at 22 UTC 20 September 1996 prior to the formation of Super Typhoon Yates. Arrow indicates MCS A.

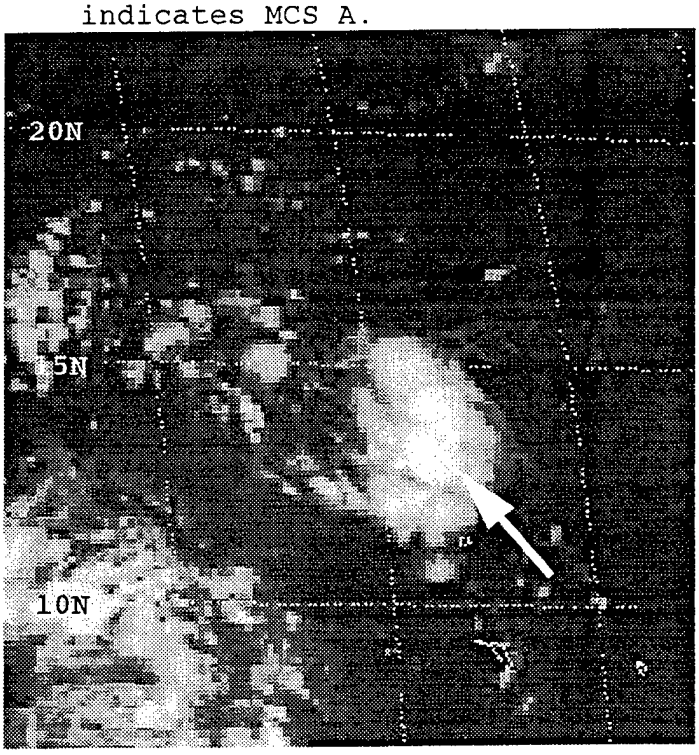

Fig. 3.A.8 As in Fig. 3.A.7, except at 18 UTC 21 September 1996. Arrow indicates thunderstorms that develop into MCS B.

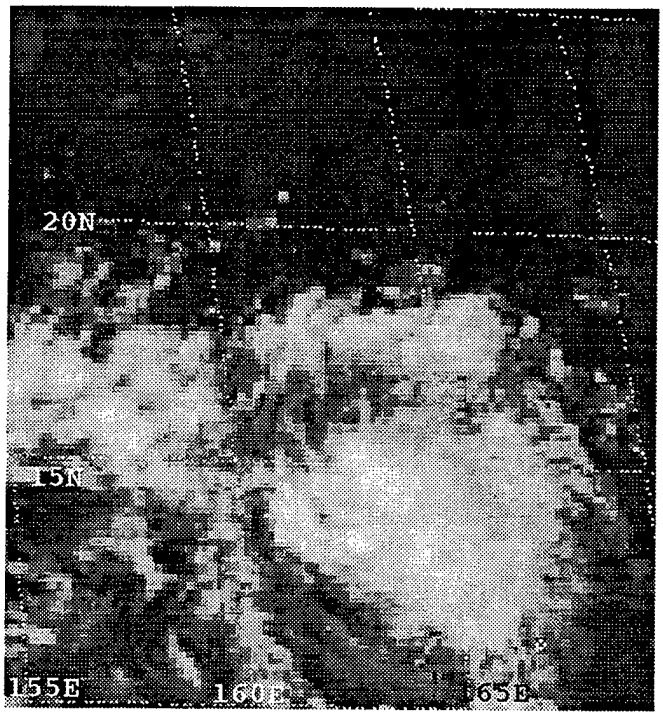

Fig. 3.A.9 As in Fig. 3.A.7, except at 04 UTC 22 September 1996.

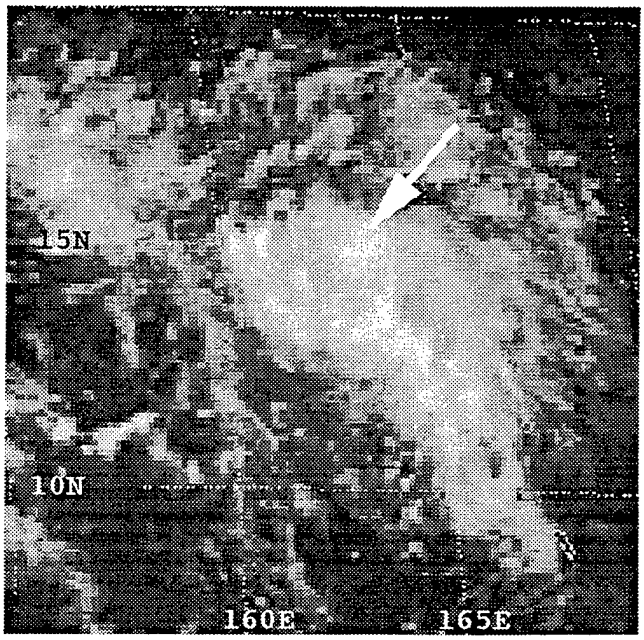

Fig. 3.A.10 As in Fig. 3.A.7, except at 06 UTC 22 September 1996. Arrow indicates thunderstorm that develops into MCS C.

UTC 22 September 1996, JTWC issued the first warning, and the system was subsequently labeled a tropical storm.

Both Typhoon Teresa and Super Typhoon Yates provide clear examples of mesoscale thermodynamic and dynamic processes being the predominant contributors to formation of a tropical cyclone with a relatively minor contribution from the synoptic-scale dynamic forcing. Table 2-1 summarizes the variables from Chapter II.B for the Ofelia-type category of tropical cyclone genesis during the pre-organization and organization stages of development. Several trends are apparent in the entries in Table 3-1.

The size of the overall cloud systems (Table 2-1, column 3) is relatively small, and no large tropical cyclones were observed to be associated with this type of formation. This is consistent with the Ofelia-type conceptual model and the space and time scales of mesoscale weather systems in the tropics. All except one of the MCSs had rapid growth (Table 2-1, column 5). In the pre-organization stage, nine of eleven MCSs also decayed rapidly. However, the MCSs tended to persist during the organization stage.

Second, 19 of the 21 MCSs developed directly over the system's low-level circulation center (Table 2-1, column 6), which was a key feature of the Ofelia development (Harr et al. 1996a). This observation indicates that the MCS activity is driving the dynamic and thermodynamic processes in the core of the Ofelia-type developing system, since synoptic-scale forcing does not seem to be contributing significantly.

Third, while 9 of 11analyzed MCSs had only a weak convective organization (column 11) during the pre-organization stage, nine of the ten MCSs during the

organization stage had well-organized convection. The repetitive occurrence of MCSs over the LLCC of the developing system increases the dynamic and thermodynamic potential of the system, especially in the inner core. While the previous MCS increases the deep-layer relative humidity by lifting water vapor from the planetary boundary layer, its upper-level outflow provides a buffer against the inhibiting influence of vertical wind shear over the inner core. Thus, each new MCS that forms over the same area is expected to be more intense and better organized than those preceding it, as seen in the increase in central updraft strength from the first pre-Teresa MCS compared to those following it.

Fourth, 19 of 21 MCSs had a rotation of the deep convective cloud elements during the MCS lifetime and / or inner spiral bands (column 9) following dissipation of the cirrus shield. This observation indicates a coupling of the system mesoscale dynamic and thermodynamic energy into a synergistic feedback loop that led to an increased system organization. This idea will be explored in greater detail in Chapter IV.

Fifth, only three of the six Ofelia-type formations occurred in association with enhanced low-level confluence and shear vorticity provided by cross-equatorial wind flow (Table 2-1, column 10). In the remaining half of the Ofelia-type cases, the critical dynamic forcing of the increased organization of the tropical system must definitely have been predominantly associated with MCS activity.

For the Ofelia-type tropical cyclone formations, the remaining variables in Table 3-1 do not have a consistent change in characteristics from the pre-organization to the organization stage that would separate them from the other formation types discussed here.

B. ROBYN-TYPE

The second pathway to tropical cyclone genesis discussed in Chapter I.C involves an increase in low-level cyclonic relative vorticity and the lowering of the surface pressure predominantly caused by synoptic processes. Whereas MCSs are present in these genesis cases, they do not play the same critical role in intensifying the system circulation as in the Ofelia-type. Only two other of the 13 formations analyzed were classified as Robyn-type cases. In this section, two specific examples of a Robyn-type case will be reviewed and the trends in the variables of this data subset of TC formations will be examined.

Super Typhoon Fred and Typhoon Zane were representative examples of this tropical cyclone genesis pathway and provide insight into the processes occurring in a synoptic-driven tropical cyclone formation. Super Typhoon Fred developed from a synoptic-scale shear zone into a large tropical cyclone during mid-August 1994 (Fig. 3.B.1). The strong cyclonic circulation early in the development of the pre-Fred tropical disturbance was remarkable. By 10 UTC 12 August 1994, the pre-Fred tropical disturbance was located at 21°N, 152°E and the cyclonic circulation of the entire system was well established (Fig. 3.B.2). Notice also the lack of organized deep convection throughout the formation stage. From 11 UTC 12 August until 05 UTC 13 August, the system drifted west- southwest to 20°N, 149°E with scattered and weakly organized thunderstorms in and around the LLCC. However, the synoptic environment was thermodynamically and dynamically favorable for tropical cyclone development. During this time, the synoptic area of cyclonic winds expanded and intensified around the tropical disturbance.

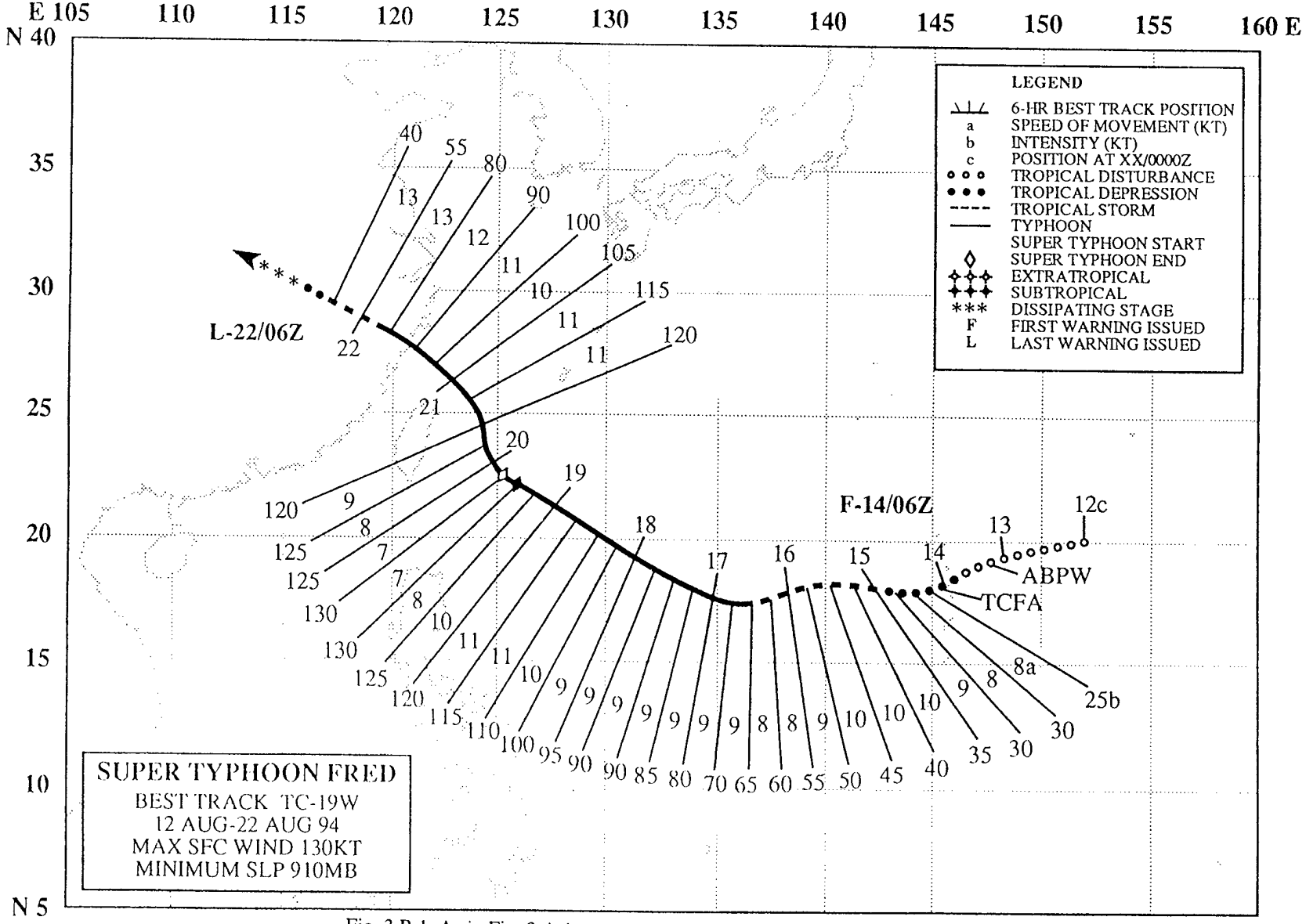

Fig. 3.B.1 As in Fig. 3.A.1, except for Super Typhoon Fred, 12-22 August 1994.

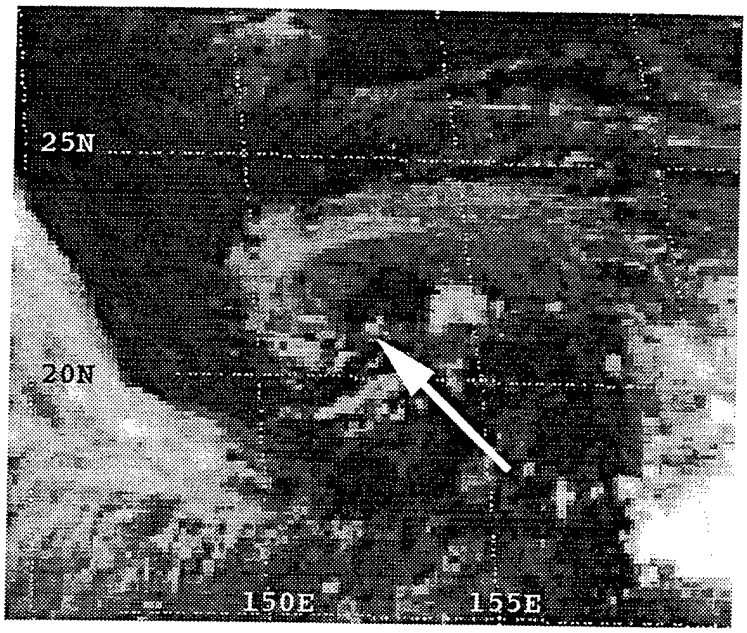

Fig. 3.B.2 As in Fig. 3.A.3, except at 10 UTC 12 August 1994 and preceding the formation of Super Typhoon Fred. Arrow indicates system LLCC.

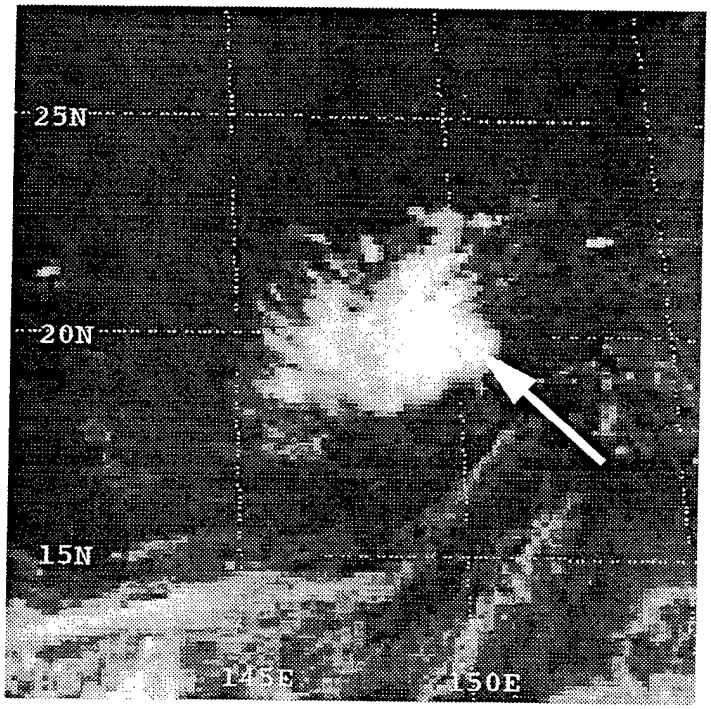

Fig 3.B.3 As in Fig. 3.B.2, except at 06 UTC 13 August 1994. Arrow indicates developing MCS.

At 06 UTC 13 August (Fig. 3.B.3), a small cluster of thunderstorms rapidly developed over the LLCC into a small, poorly organized MCS, which is identified in Table 2-2 as MCS A. However, the MCS convection rapidly collapsed and the resulting MCV disappeared or was quickly absorbed into the powerful pre-existing LLCC. Because of the short time and small space scales of MCS A, and lack of a vigorous updraft, MCS A is not considered to be an important contributor to the development of the pre-Fred tropical disturbance.

From the collapse of MCS A starting at 14 UTC 13 August (Fig. 3.B.4) until the first warning issued by Joint Typhoon Warning Center at 06 UTC 14 August, scattered thunderstorms were observed over the LLCC, but without MCS activity. It was not until 09 UTC 14 August (Fig. 3.B.5)—three hours after JTWC classified it as a tropical storm—that thunderstorms began to develop and merge into a second, larger MCS labeled MCS B. Until this time, the system appeared to be forced predominantly by the synoptic-scale inflow.

Typhoon Zane provides another example of synoptic-scale processes being the predominant contributor to tropical cyclone formation. Typhoon Zane developed from a monsoon depression into a large tropical cyclone in the western North Pacific during late September 1996 (Fig. 3.B.6). The pre-Zane tropical disturbance formed near the equator. By 04 UTC 20 September 1996, a MCS (labeled MCS A in Table 2-2) was located at 8°N, 160°E (Fig. 3.B.7). The synoptic environment was thermodynamically favorable and—due to the presence of a cyclonic wind shear zone—soon became dynamically very favorable for convection. These conditions intensified as the system drifted west and then northwest.

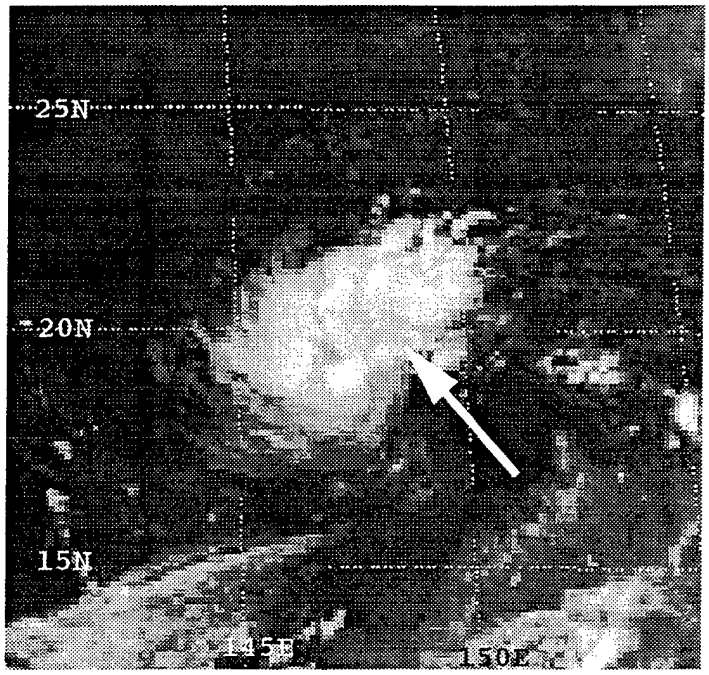

Fig. 3.B.4 As in Fig. 3.B.2, except at 14 UTC 13 August 1994. Arrow indicates collapsing MCS A.

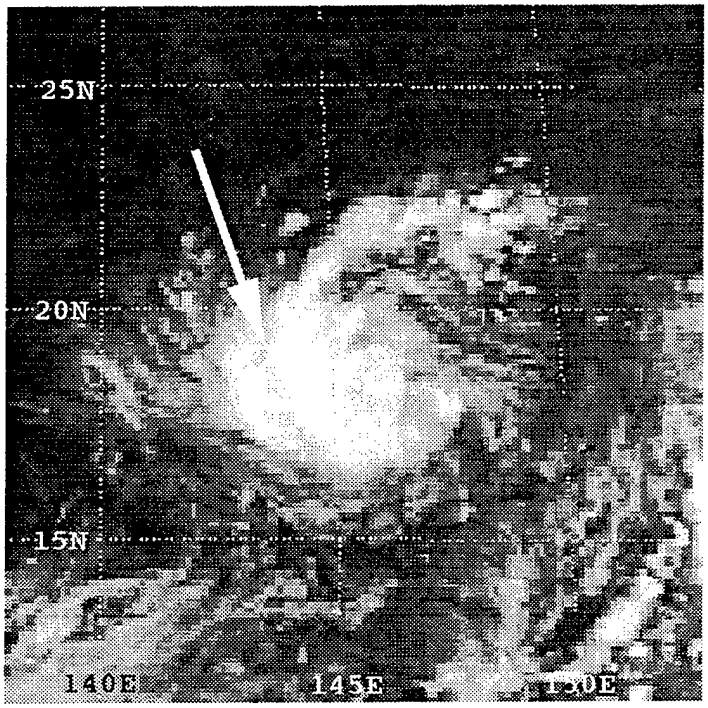

Fig. 3.B.5 As in Fig. 3.B.2, except at 09 UTC 14 August 1994. Arrow indicates MCS B.

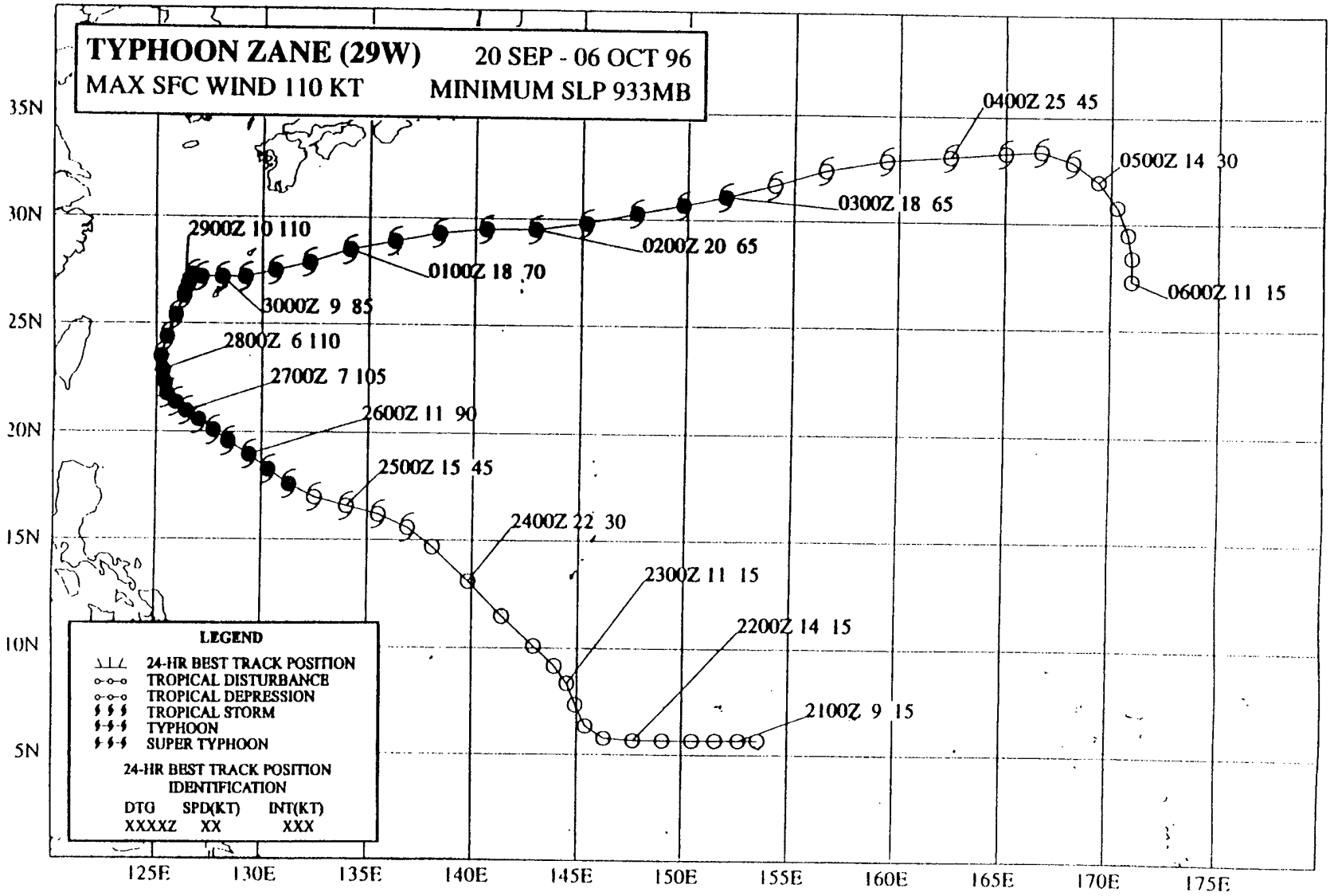

Fig. 3.B.6 As in Fig. 3.A.1, except for Typhoon Zane, 20 September - 6 October 1996.

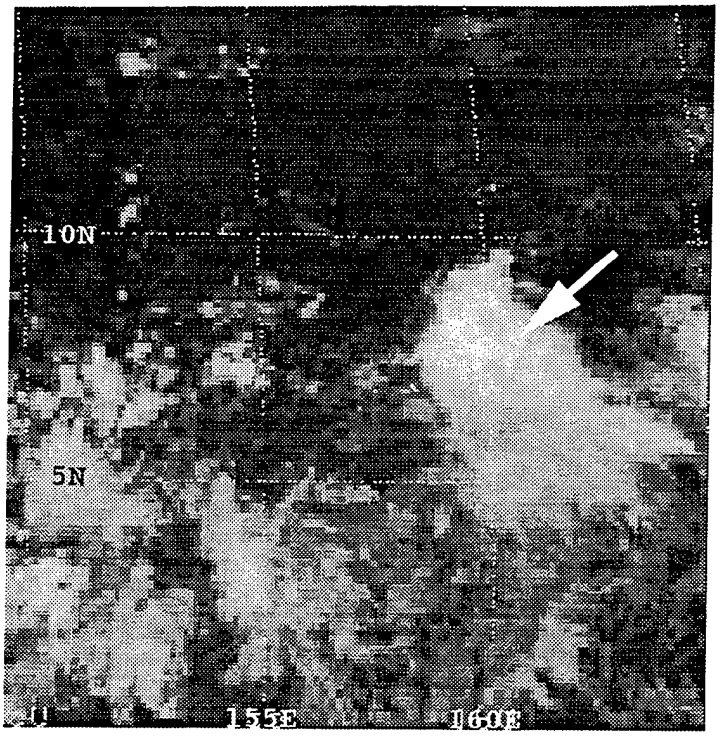

Fig. 3.B.7 As in Fig. 3.B.2, except at 04 UTC 20 September 1996 and prior to the formation of Typhoon Zane. Arrow indicates MCS A.

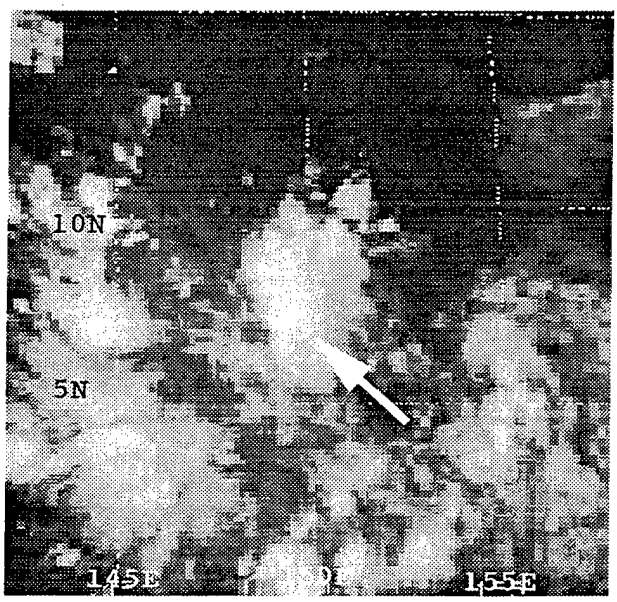

Fig. 3.B.8 As in Fig. 3.B.7, except at 11 UTC 20 September 1996. Arrow indicates MCS B.

From 05 UTC to 12 UTC 20 September, MCS A gradually collapsed while a large but peripheral MCS, labeled MCS B, began to develop to the west at 7°N, 150°E (Fig. 3.B.8). While MCS B dissipated without appearing to generate a MCV, by 18 UTC 20 September a LLCC appeared where MCS A collapsed (Fig. 3.B.9). This LLCC was positioned at 5°N, 155°E along the axis of a weak synoptic shear zone and appeared to be strengthened by the shear zone as the LLCC advected west. Since the LLCC was at a relatively low latitude, this was not considered to be dynamically favorable for formation.

By 06 UTC 21 September, a large area of deep convection composed of numerous individual thunderstorms developed from the south through the east of the LLCC (Fig. 3.B.10). By 15 UTC 21 September, they formed a large but weakly organized MCS (labeled MCS C) east of the LLCC (Fig. 3.B.11). However, MCS C dissipated by 18 UTC 21 September and the LLCC was advected to the western edge of the monsoon depression.

From 19 UTC 21 September until 15 UTC 22 September, the system remained convectively dormant. At 16 UTC 22 September, a large MCS (labeled MCS D) began to grow near 6°N, 149°E (Fig. 3.B.12). After its collapse at 22 UTC 22 September, and the dissipation of its cirrus shield at 05 UTC 23 September (Fig. 3.B.13), a broad, slowly rotating LLCC was observed centered at 7°N, 146°E. Simultaneously, a burst of cross-equatorial flow strengthened the LLCC and deflected it from a westward drift toward the north-northwest. This wind burst originated far to the southwest of the monsoon depression and appeared to contribute to a rapid organization of the tropical disturbance. Displacement of the system towards higher latitudes—accompanied by an increase in the Coriolis parameter—also indicates a more dynamically favorable synoptic environment.

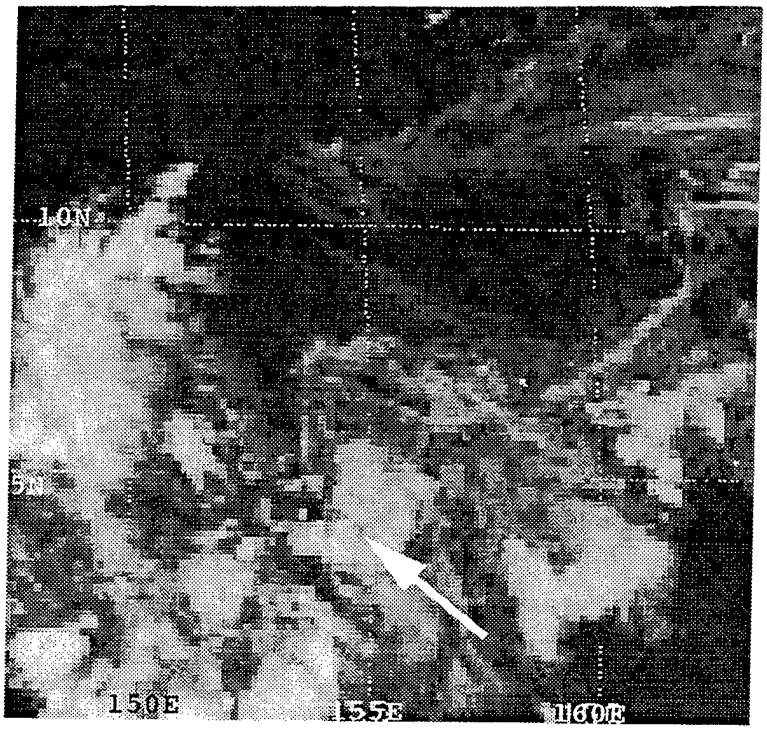

Fig. 3.B.9 As in Fig. 3.B.7, except at 18 UTC 20 September 1996. Arrow indicates system LLCC.

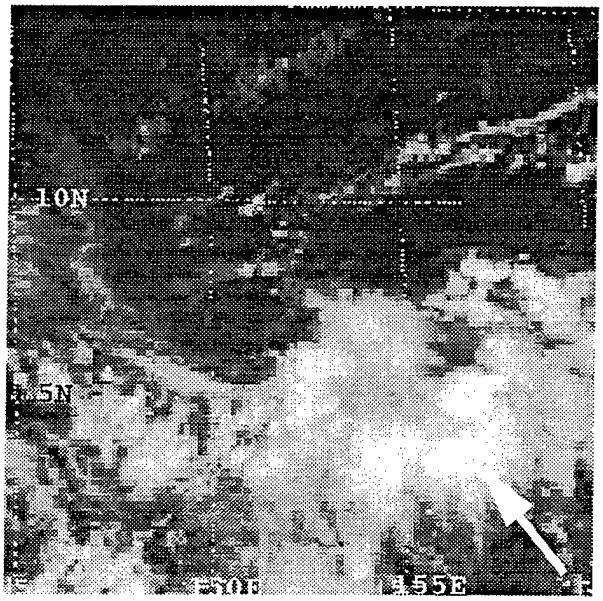

Fig. 3.B.10 As in Fig. 3.B.7, except at 06 UTC 21 September 1996. Arrow indicates thunderstorms that develop into MCS C.

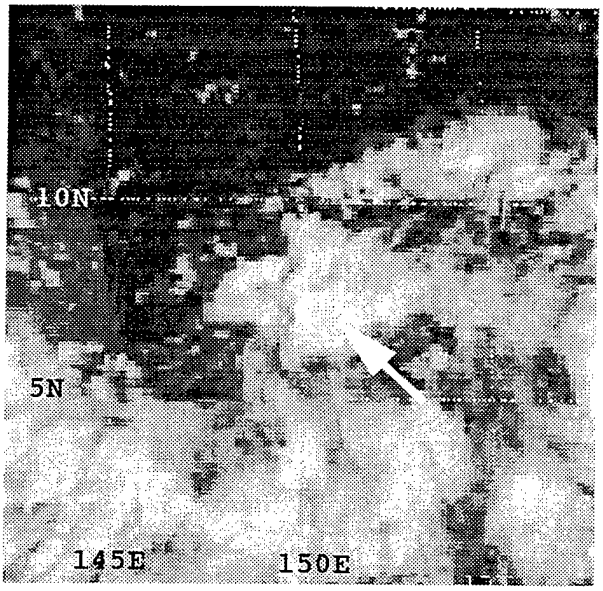

Fig. 3.B.11 As in Fig. 3.B.7, except at 15 UTC 21 September 1996. Arrow indicates MCS C.

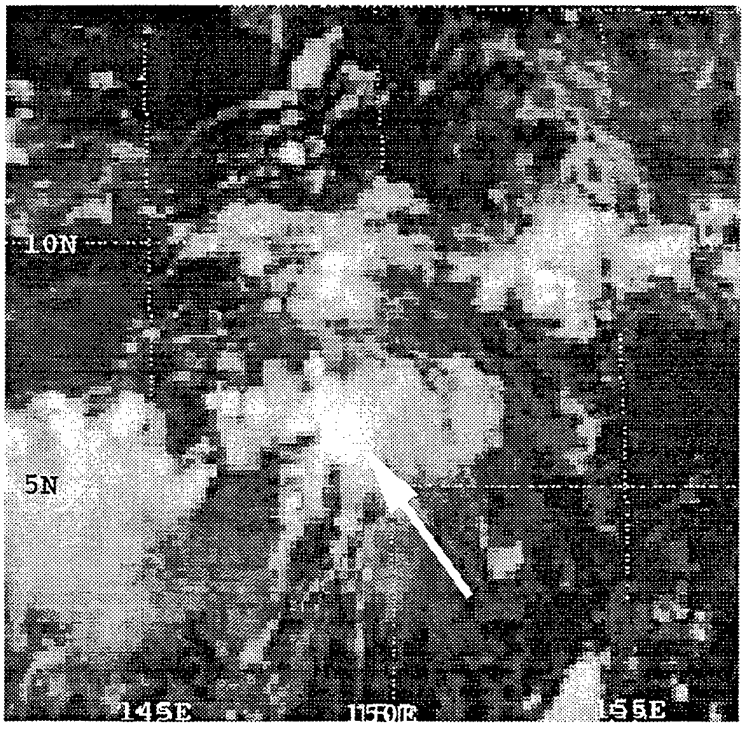

Fig. 3.B.12 As in Fig. 3.B.7, except at 16 UTC 22 September 1996. Arrow indicates thunderstorms that developed into MCS D.

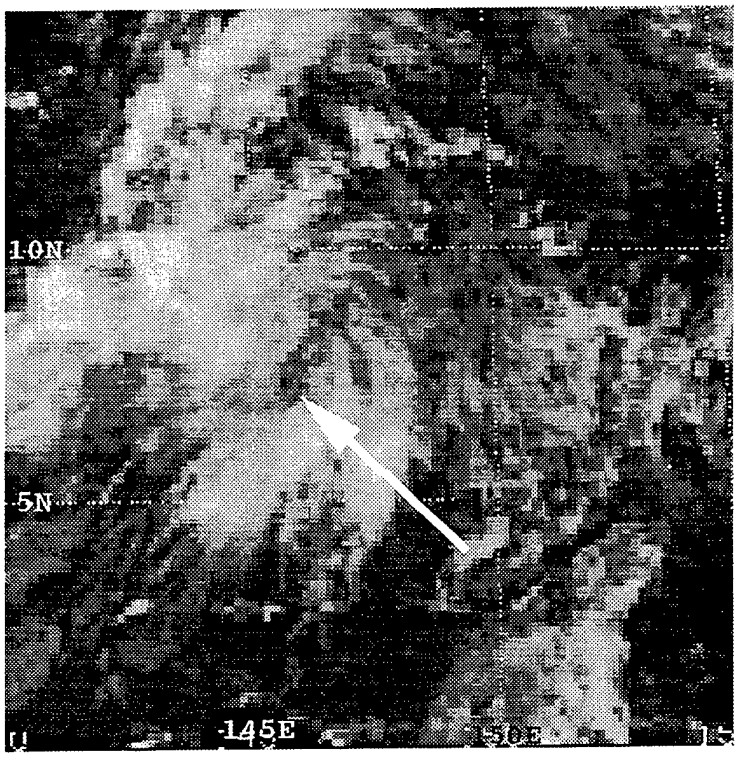

Fig. 3.B.13 As in Fig. 3.B.7, except at 05 UTC 23 September 1996. Arrow indicates system LLCC.

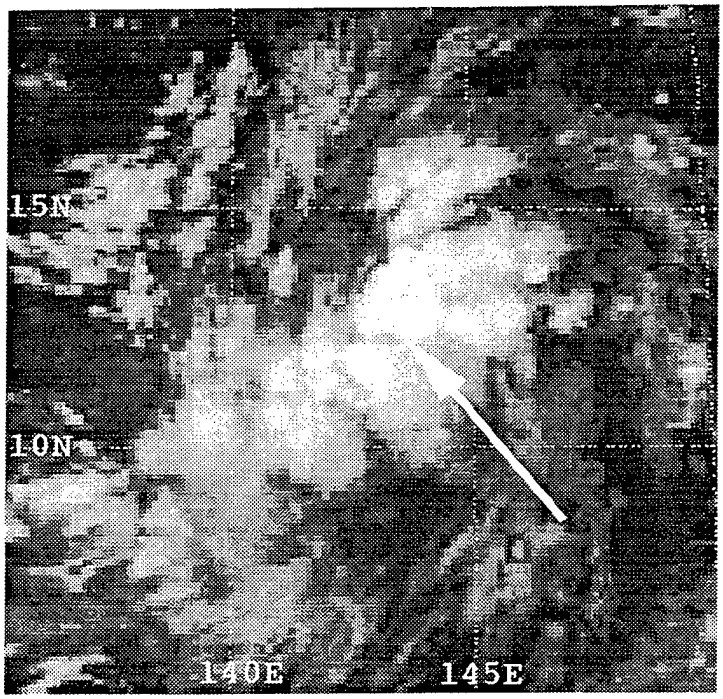

Fig. 3.B.14 12 UTC 23 Sep 1996 Arrow indicates MCS E.

The cross-equatorial flow advected the LLCC northward toward a cluster of growing thunderstorms that by 12 UTC 23 September had become a loosely organized MCS, labeled MCS E (Fig. 3.B.14). By 20 UTC 23 September, the LLCC was co-located with MCS E, which increased both the intensity and the areal extent of the MCS. Although MCS E collapsed after 02 UTC 24 September, the cirrus shield was rotating anticyclonically (Fig. 3.B.15). A new MCS (labeled MCS F) quickly developed over the LLCC and the Joint Typhoon Warning Center classified the system as a tropical storm at 12 UTC 24 September 1996.

Super Typhoon Fred and Typhoon Zane both provide examples of synoptic-scale dynamic processes in a thermodynamically favorable environment as the predominant contributor to the formation of a tropical cyclone. Table 2-2 summarizes the variables from Chapter II.B for the Robyn-type category of tropical cyclone genesis during the pre-organization and organization stages. Although trends are difficult to establish because of the small sample size, several trends are apparent from the entries in Table 2-2.

First, the resulting tropical cyclones are relatively large (Table 2-2, column 3). No small tropical cyclones were observed to be associated with this type of formation. This is consistent with the Robyn-type conceptual model (Harr et al. 1996b) and the space and time scales of synoptic-scale processes.

Second, nine of 11 MCSs occurred in conjunction with concentrated low-level confluence and cyclonic shear vorticity of cross-equatorial wind flow (Table 2-2, column 10). For the Robyn-type tropical cyclone formations, the remaining variables in Table 2-2 do not show a consistent change in characteristics between the pre-organization and

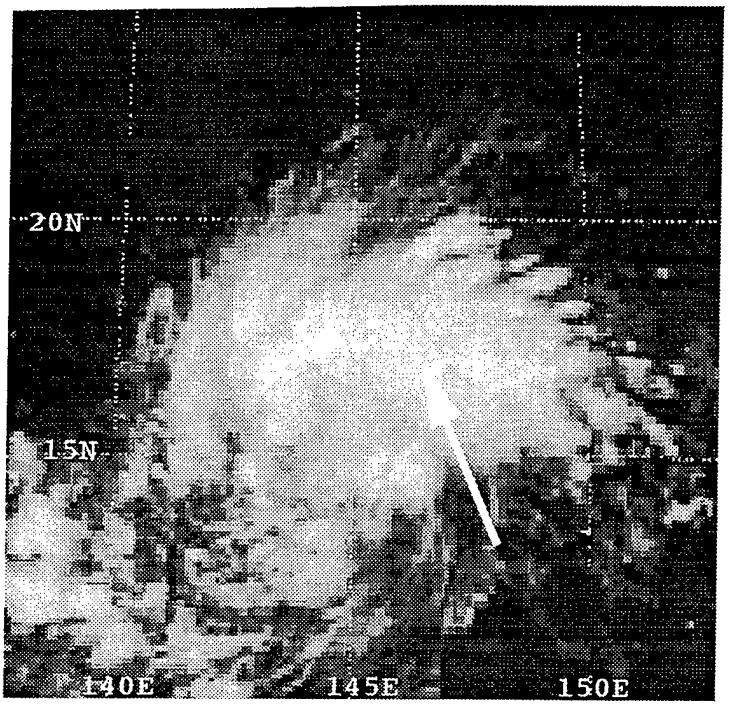

Fig. 3.B.15 As in Fig. 3.B.7, except at 02 UTC 24 September 1996. Arrow indicates collapsing MCS E.

organization stage that would separate them from the other formation types discussed here.

C. COMBINATION-TYPE

A third pathway to tropical cyclone genesis is proposed because five of the 13 cases were not clearly separable into either the Ofelia- or Robyn-type conceptual models. These cases had significant contributions to their development from both mesoscale convective systems and synoptic-scale dynamic forcing, and it was not possible to determine accurately which process was more important to the TC formation. These cases were labeled Combination formations and are summarized in Table 2-3. In this section, two specific examples of a Combination-type case will be reviewed and the trends in the variables in this subset of TC formations will be examined.

Typhoon Sibyl and Typhoon Kinna were representative cases and provide insights into the processes occurring in a combined mesoscale- and synoptic-driven tropical cyclone genesis. Typhoon Sibyl developed from an equatorial wave into a large TC in the western North Pacific during late September 1995 (Fig. 3.C.1). The pre-Sibyl tropical disturbance formed near the equator east of the monsoon trough and by 17 UTC 22 September 1995 was located at 6°N, 167°E. A large MCS, which is identified as MCS A in Table 2-3, formed at 6^0N, 164^0E near the system center. Although the synoptic environment was thermodynamically favorable for convection, it is considered to be only weakly dynamically favorable for convection because of the low values of Coriolis and relative vorticity, and cross-equatorial flow was not evident in the early stages of development.

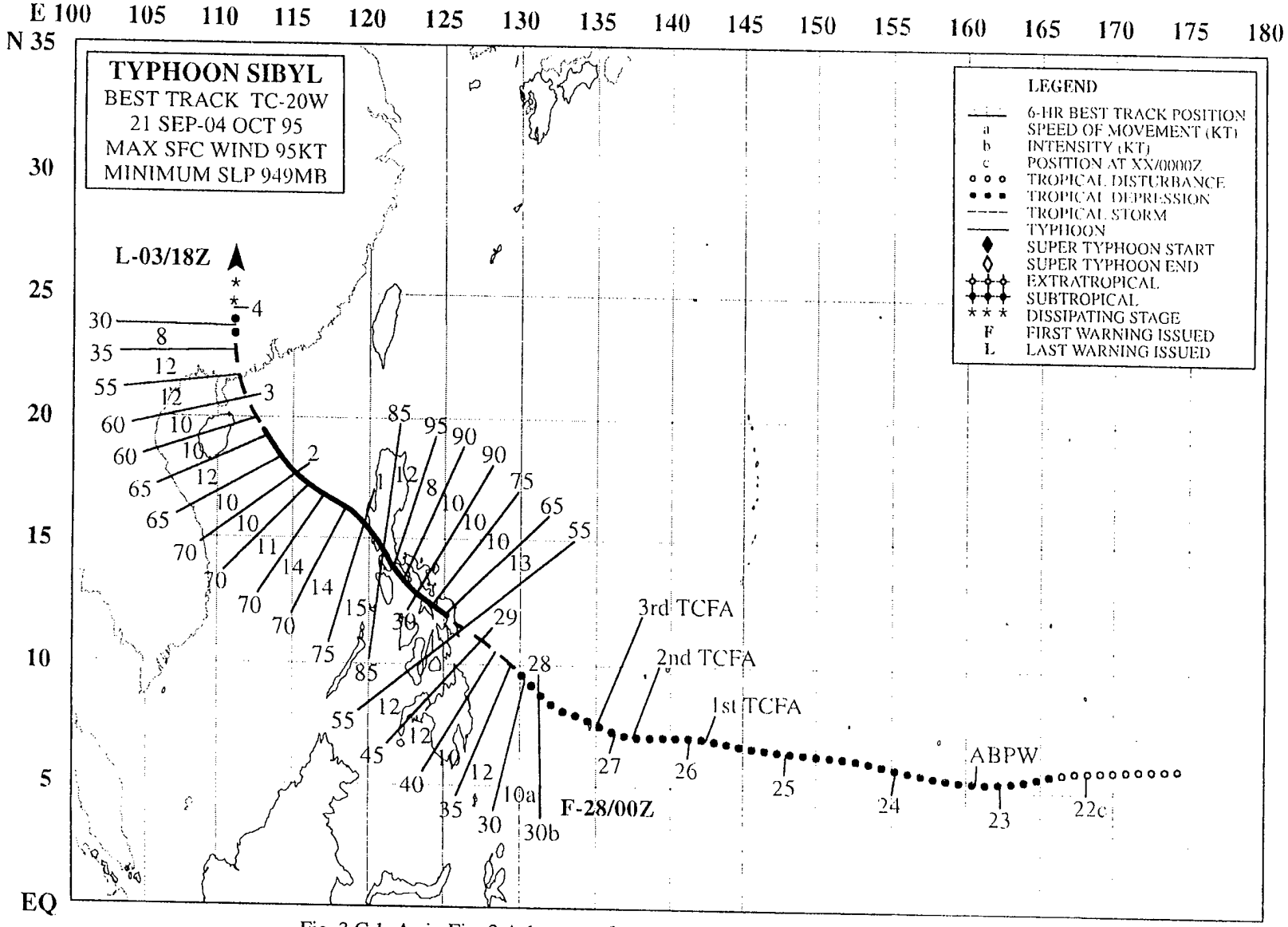

Fig. 3.C.1 As in Fig. 3.A.1, except for Typhoon Sibyl, 21 September - 4 October 1995.

By 00 UTC 23 September (Fig. 3.C.2), MCS A collapsed and the LLCC was visible as the cirrus shield dissipated. For the next 35 hours until 12 UTC 24 September, the system deep convection was at a minimum and contained only scattered and weakly organized thunderstorms. No satellite imagery was available for the period of 13 - 15 UTC 24 September. At 16 UTC, a MCS, which is labeled MCS B, developed near 3°N, 146°E (Fig. 3.C.3). This MCS dissipated by 02 UTC 25 September and did not create a long-lived LLCC.

Clusters of thunderstorms began to organize by 09 UTC 25 September into two MCSs at 4°N, 140°E and 5°N, 146°E (Fig. 3.C.4). The weakly organized MCS to the west, which is labeled C in Table 2-3, quickly dissipated without any apparent effect on the system circulation. However, the second MCS (labeled D) was centrally located with respect to the LLCC and persisted until 06 UTC 26 September. As its cirrus shield dissipated, the cumulus lines spiraling into the LLCC were more tightly curved and the circulation expanded from the LLCC to encompass the entire tropical disturbance (Fig. 3.C.5). Simultaneously, the synoptic forcing changed. A burst of cross-equatorial flow to the east of the system center was evident in the imagery from 11 UTC 25 September - 8 UTC 26 September, which provided an environment of low-level confluence and cyclonic shear vorticity. Strong cross-equatorial flow was a consistent feature during the remainder of the formation stage.

At 22 UTC 26 September, a large MCS (labeled E) with a vigorous updraft formed near 9°N, 135°E and rotated around the LLCC (Fig. 3.C.6). Although JTWC did not classify the system as a tropical storm until 12 UTC 28 September, it had all of the characteristics of a tropical storm at this earlier time. That is, the cyclonic circulation is

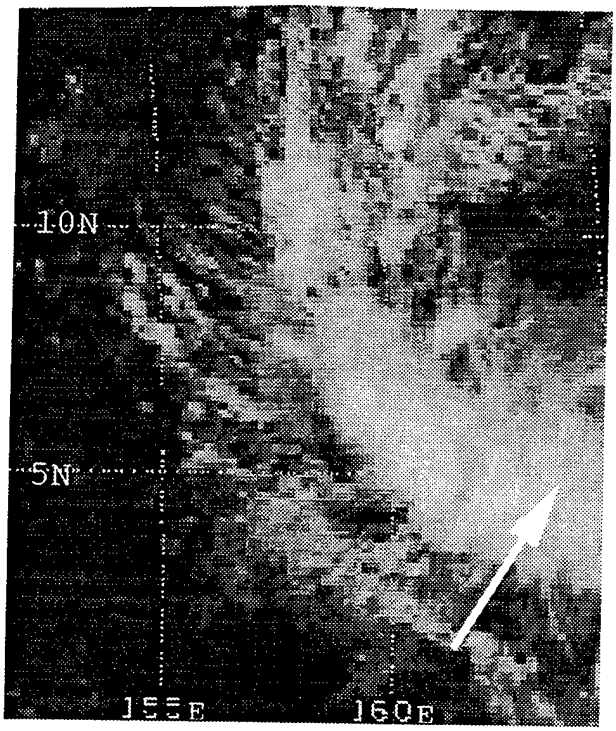

Fig. 3.C.2 00 UTC 23 Sep 1995
Arrow indicates system LLCC.

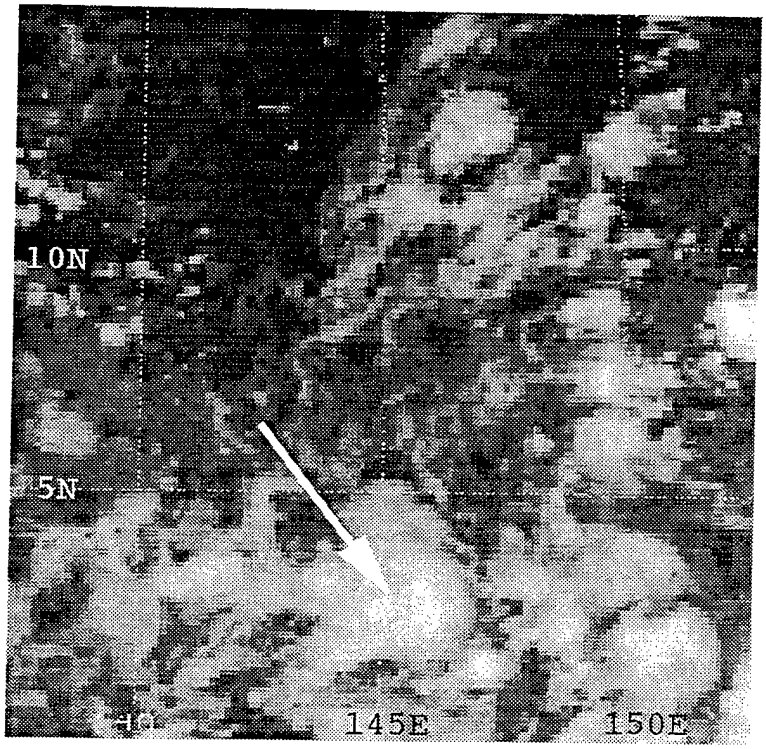

Fig. 3.C.3 16 UTC 24 Sep 1995
Arrow indicates MCS B.

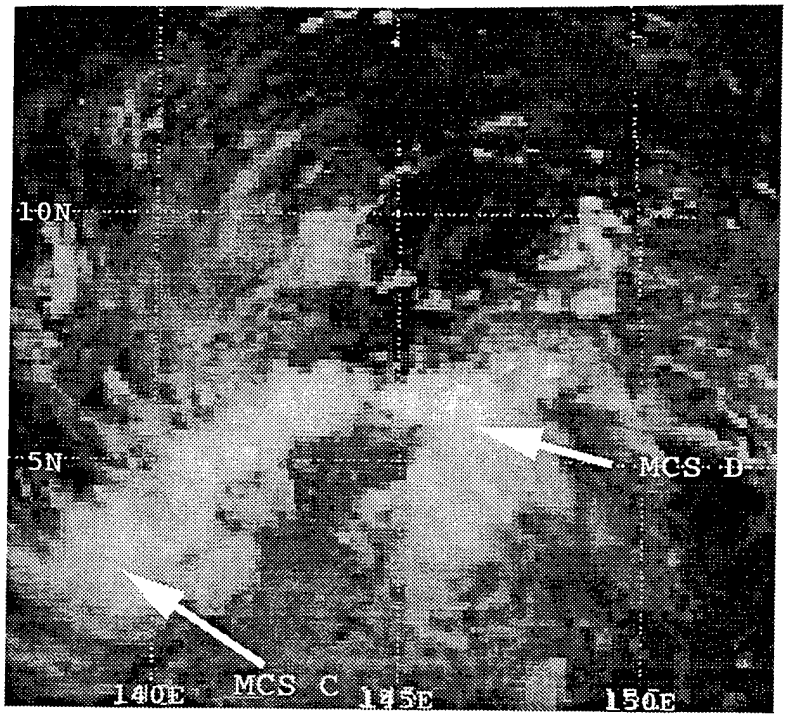

Fig. 3.C.4.As in Fig. 3.C.2, except at 12 UTC 25 September 1995. Arrows indicate MCS C and MCS D.

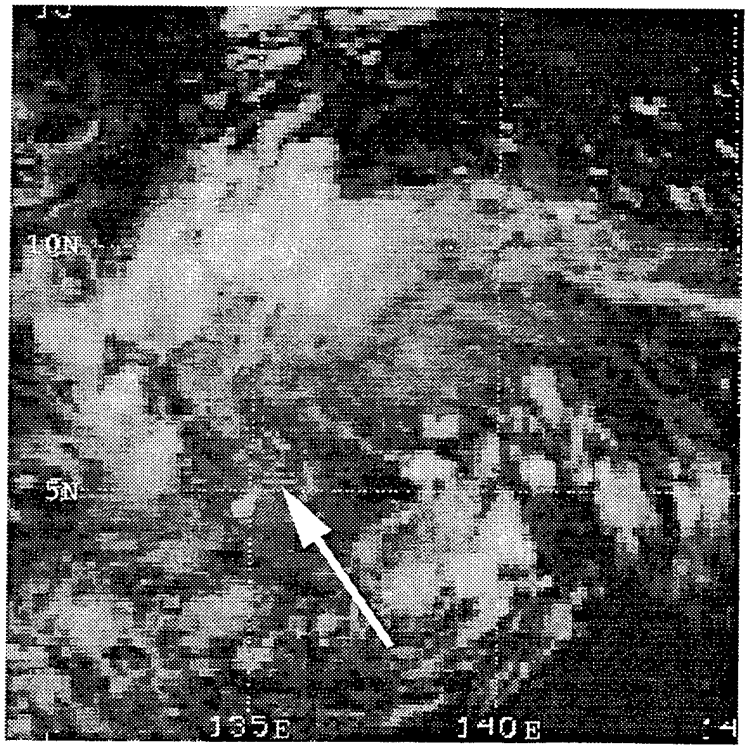

Fig. 3.C.5 As in Fig. 3.C.2, except at 09 UTC 26 September 1995. Arrow indicates system LLCC.

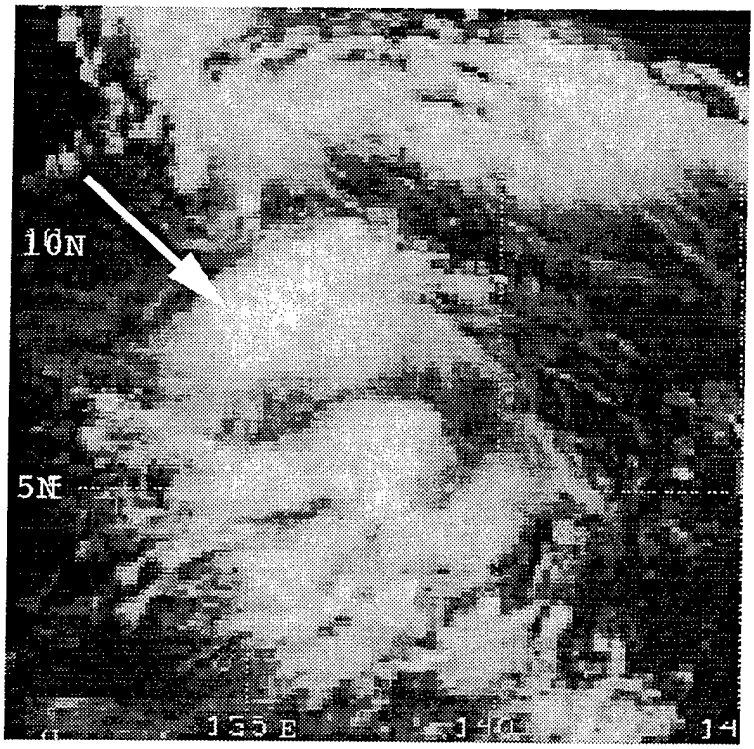

Fig. 3.C.6 00 UTC 27 Sep 1995
Arrow indicates MCS E.

strong and established throughout the entire system, continuous deep convection exists over the LLCC, and an extensive anticyclonic outflow region exists aloft.

Typhoon Sibyl was categorized as a Combination-type TC formation because of its mixture of mesoscale and synoptic-scale forcing. The original LLCC about which the system later developed was created by MCS activity and sustained for several days when the synoptic dynamic forcing appeared weak. The occurrence and central location of MCS D appeared to play a significant role in increasing the rotation of the LLCC prior to the advent of cross-equatorial flow. Additional synoptic dynamical forcing—in the form of a larger Coriolis parameter—acted on the system as it drifted north. During the most pronounced period of increasing organization, the synoptic forcing provided by cross-equatorial winds contributed to the spin up of the system circulation and thus to the transformation of the tropical disturbance into a tropical storm.

Typhoon Kinna developed from a monsoon depression into a tropical cyclone in the western North Pacific during early September 1994 (Fig. 3.C.7). The pre-Kinna tropical disturbance formed east of Guam and by 18 UTC 2 September 1994—when the first imagery became available—consisted of two MCSs and scattered thunderstorms (Fig. 3.C.8). At this time, the environment was thermodynamically and dynamically favorable for convection, with strong westerlies south of the monsoon depression providing cyclonic shear vorticity. The northern MCS, which is labeled MCS A in Table 2-3, was weakly organized and quickly dissipated, apparently without creating a MCV. The southwestern MCS, labeled MCS B, also dissipated rapidly, but by 23 UTC 2 September it had formed a LLCC that was visible near 15°N, 147°E (Fig. 3.C.9). For the next several hours, this LLCC drifted north with only scattered thunderstorm activity. At

Fig. 3.C.7 As in Fig. 3.A.1, except for Typhoon Kinna, 1-12 September 1994.

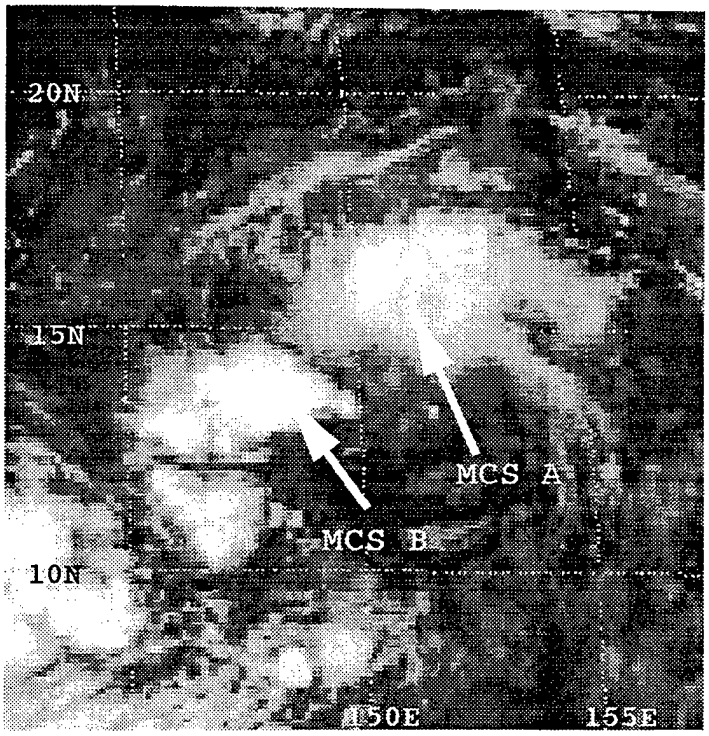

Fig. 3.C.8 As in Fig. 3.C.2, except at 18 UTC 2 September 1994 prior to the formation of Typhoon Kinna. Arrows indicate MCS A and MCS B.

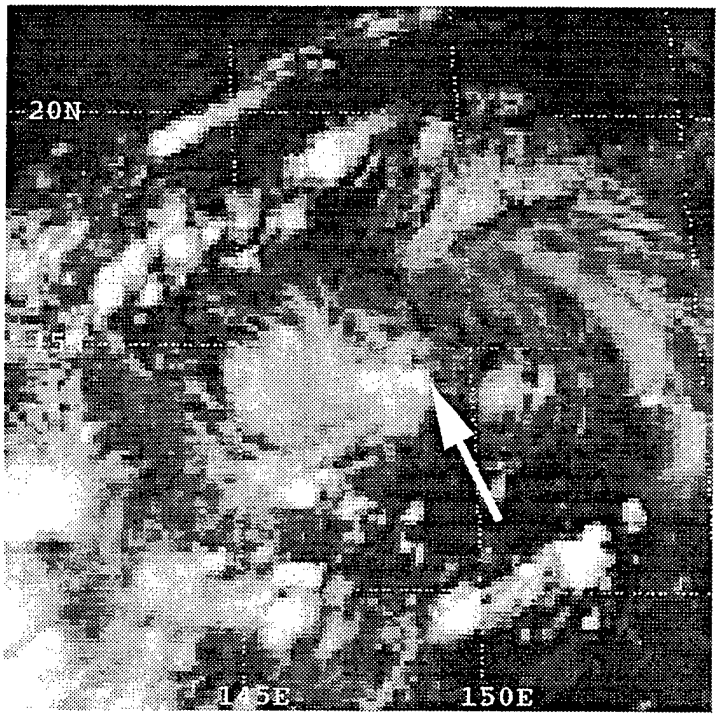

Fig. 3.C.9 As in Fig. 3.C.8, except at 23 UTC 2 September 1994. Arrow indicates system LLCC.

07 UTC 3 September, a cluster of thunderstorms near the LLCC developed into a multi-celled MCS, labeled C, at 17°N, 147°E (Fig. 3.C.10).

The dissipation of MCS C through 16 UTC 3 September resulted in a large, roughly, circular cloud-minimum hole and an outflow boundary (Fig. 3.C.11). The low-level convergence of this expanding outflow boundary triggered the development at 20 UTC 3 September of a weakly organized, multi-celled MCS near 15°N, 148°E (Fig. 3.C.12). However, this peripheral MCS (labeled MCS D) dissipated without an apparent contribution to the developing system.

At 03 UTC 4 September, a line of convection oriented southwest to northeast developed with a MCS (labeled MCS E) that generated with its southwestern end directly over the LLCC at 19°N, 144°E (Fig. 3.C.13). Upon the collapse of MCS E at 11 UTC 4 September, the LLCC continued its northward movement. By 16 UTC 4 September, the outflow boundary of MCS E appeared to trigger the growth of a large peripheral MCS (labeled MCS F) near 19°N, 146°E (Fig. 3.C.14). As MCS F dissipated at 02 UTC 5 September, its outflow boundary contributed to the growth of a MCS (labeled MCS G) southeast of the LLCC (Fig. 3.C.15). By then, rotation of the system was evident and a new MCS (labeled MCS H) developed over the LLCC (Fig. 3.C.16) at 06 UTC 5 September 1994. At this time, JTWC classified the system as a tropical storm.

Typhoon Kinna was categorized as a Combination-type formation because of its mixture of mesoscale and synoptic forcing processes. The repeated MCS developments were supported by synoptic-scale wind flow originating outside the system. The low-level confluence and cyclonic shear vorticity further enhanced the mesoscale processes.

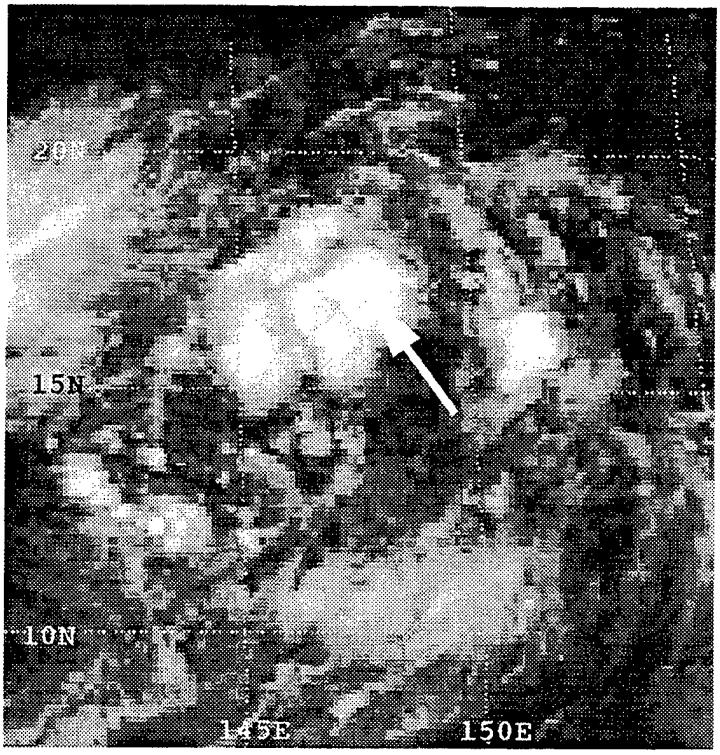

Fig. 3.C.10 As in Fig. 3.C.8, except at 7 UTC 3 September 1994. Arrow indicates MCS C.

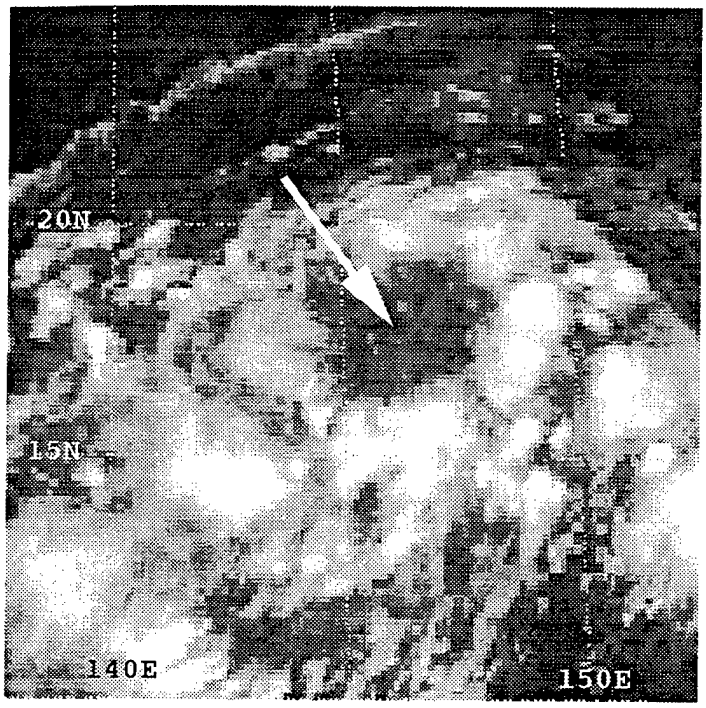

Fig. 3.C.11 As in Fig. 3.C.8, except at 17 UTC 3 September 1994. Arrow indicates cloud-minimum hole surrounded by convection.

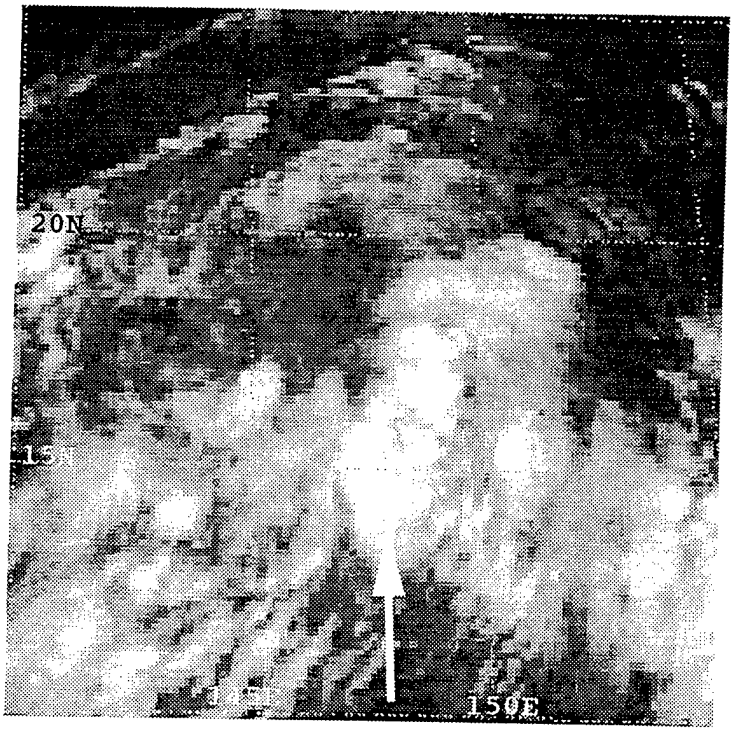

Fig. 3.C.12 As in Fig. 3.C.8, except at 20 UTC 3 September 1994. Arrow indicates MCS D.

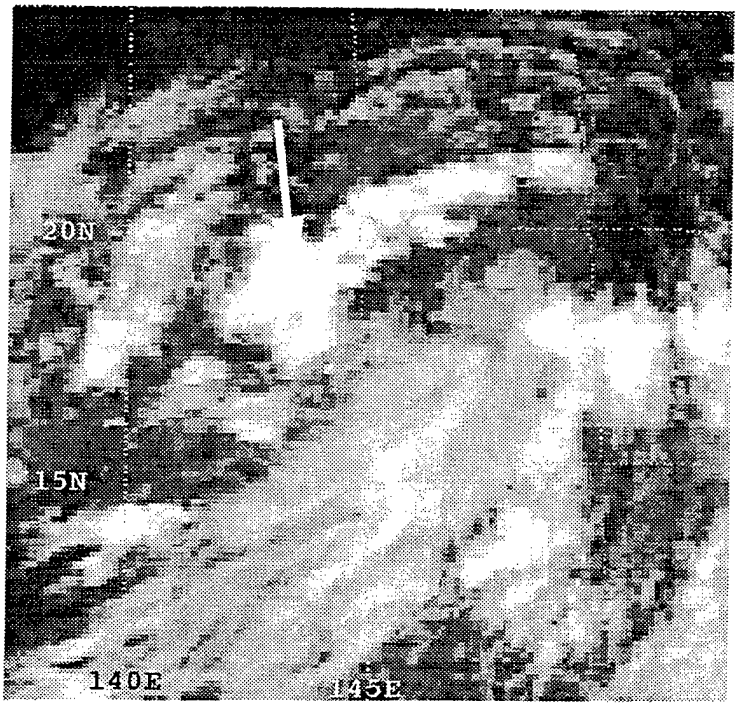

Fig. 3.C.13 As in Fig. 3.C.8, except at 04 UTC 4 September 1994. Arrow indicates MCS E.

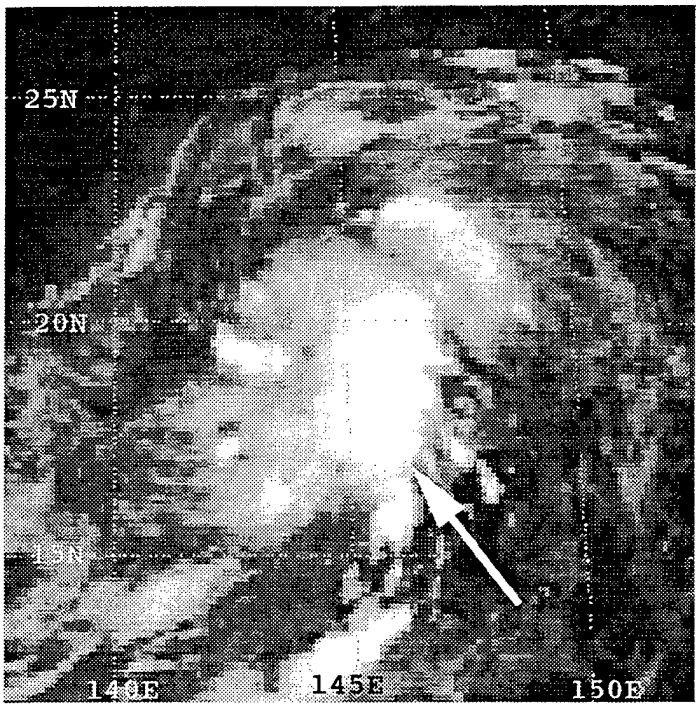

Fig. 3.C.14 As in Fig. 3.C.8, except at 16 UTC 4 September 1994. Arrow indicates MCS F.

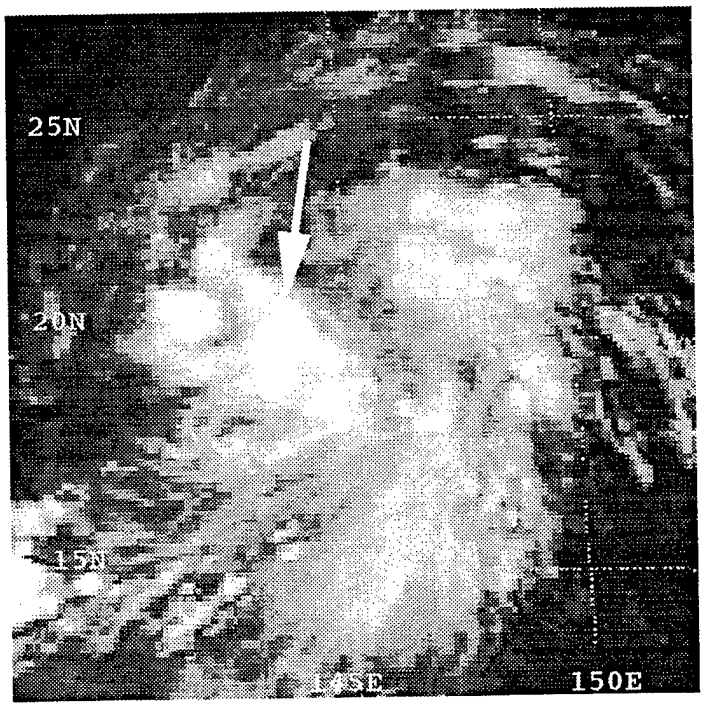

Fig. 3.C.15 As in Fig. 3.C.8, except at 02 UTC 5 September 1994. Arrow indicates MCS G.

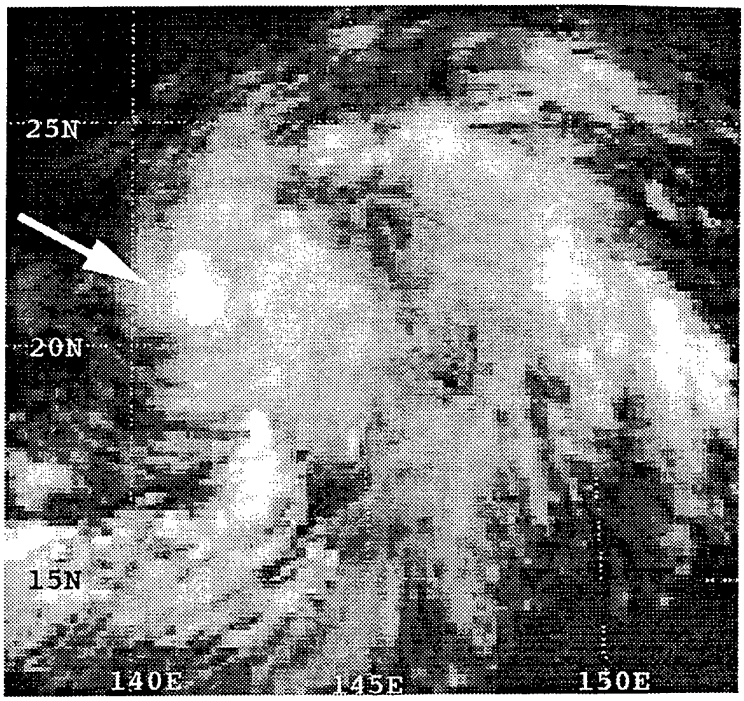

Fig. 3.C.16 As in Fig. 3.C.8, except at 06 UTC 5 September 1994. Arrow indicates MCS H.

Table 2-3 summarizes the variables from Chapter II.B for the Combination-type category of tropical cyclone genesis during the pre-organization and organization stages. In contrast to several trends in the mesoscale- or synoptic-scale processes observed for the Ofelia-type or Robyn-type formations, neither scale is clearly dominant in any of the variables for this category. The conclusion is that in some tropical cyclone formations, different space- and time-scale dynamic processes are contributing to the same result, namely, an increase in the tropical system low-level cyclonic vorticity.

In analyzing 13 tropical cyclone formations, no cases were observed of a straight-line wind surge into the center of a tropical disturbance—the mechanism proposed by Zehr (1992) as being the trigger of convective development. Straight-line wind surges, often in the form of cross-equatorial flow, did occur and were sometimes instrumental in increasing the low-level cyclonic vorticity of a developing system (e.g., in the Super Typhoon Fred case). However, they did not penetrate to the core of the system. Commonly, the higher winds passed to the side of the tropical disturbance that provided the most cyclonic shear vorticity (i.e., southerly winds on the east side of the system, westerly winds on the south side of the system). Thus, this sample of 13 cases does not support the Zehr two-stage hypothesis that states that the mechanism for renewed deep convection is a straight-line wind surge into the system center.

IV. AN ALTERNATE APPROACH

During the analysis of this dataset, it became apparent that an alternate view of the process of tropical cyclone genesis was possible that did not contrast mesoscale and synoptic forcing. The original intent was to describe objectively the transition from an unorganized tropical disturbance to an organized tropical depression. In this alternate approach, two development stages in a severe tropical cyclone are defined as a multi-dimensional organization of anomalous dynamic and thermodynamic components in a favorable synoptic environment. After defining these components, a set of possible combinations of anomalous components is proposed that may result in system organization ranging from a short-lived tropical disturbance to a severe tropical cyclone.

In the alternate approach, five dynamic or thermodynamic anomalous components are defined, each of which consists of one or more features that differ significantly relative to the normal tropical environment. These anomalies, or sets of anomalies, are either visible in, or can be inferred from animations of hourly geostationary satellite imagery. They are: (i) a dynamic component that is oriented around a vertical axis, and consists of cyclonic curvature in the lower-tropospheric wind field, and lowered pressure around a circulation center; (ii) a thermodynamic component that consists of significantly increased temperature, upward motion, and increased moisture throughout a vertical column; (iii) a time component that is defined as an extended duration (a minimum of 18 hours) of either the thermodynamic or the dynamic anomaly component; (iv) a dynamic component in the upper troposphere, which is oriented around a vertical axis, and consists of anticyclonic curvature in the wind field; and (v) a dynamic component that consists of subsiding motion and decreased moisture in a vertical column at the system core.

A severe tropical cyclone is defined to be a circulation with these five anomalous components organized into a series of interconnected feedback loops that increase the system circulation up to the limit imposed by the thermodynamic and dynamic limits of the synoptic environment. The basic building blocks of this severe tropical cyclone exist long before the development of the cyclone eye, and each fundamental building block has exactly one anomalous component. They are the low-level circulation center (component i) and the mesoscale convective system (component ii). An unorganized tropical disturbance may create one or many short-lived (less than 18 hours) LLCCs and MCSs within its broad area of convection and cyclonic wind flow. In this context, a LLCC is defined as a circulation feature that is of sufficient diameter to be identifiable on hourly satellite imagery by the axisymmetric cyclonic rotation of its low- and/or mid-level cloud elements.

It should be noted that these basic building blocks may be created by either mesoscale or synoptic processes or by both acting in concert. A mesoscale convective vortex generated in the stratiform rain area of a MCS may extend down into the planetary boundary layer and become a LLCC. By the same token, the low-level convergence of a mesoscale LLCC may generate a MCS close to or directly over it. A synoptic-scale region of enhanced shear or curvature vorticity may create an area ofcyclonic winds that becomes a persistent LLCC, and a region in which a supercell or multicell thunderstorm breaks through an inversion into an unstable layer may lead to the formation of a MCS.

The difference between an unorganized tropical disturbance and an organized tropical depression is not determined by the number of short-lived, single-component features within it, but whether it is able to generate a structure that has two of these

components. This is hypothesized to be possible in the following variations: (a) a LLCC (or the merger of two LLCCs) that exists for longer than 18 hours has a dynamical component (i) and a time component (iii); (b) a MCS that exists for longer than 18 hours has a thermodynamic component (ii) and a time component (iii); or (c) a short-lived (less than 18 hours) co-location of a MCS over a LLCC has a dynamical component (i) and a thermodynamic component (ii). In variation (c), the LLCC may be short-lived or persistent and the organization still consists of only two components because the time component requires that all anomalies persist longer than 18 hours, whereas here the MCS does not. No persistent (greater than 18 h) MCSs were observed in this data set that were associated with tropical systems of less than tropical storm strength.

To continue the alternate approach beyond the tropical cyclogenesis stage, an organized tropical depression is defined to become a tropical storm when a persistent LLCC is co-located with a single persistent MCS or continuous multiple MCSs. That is, the system would then consist of at least three components—(i) dynamical, (ii) thermodynamic, and (iii) time, and possibly an upper-tropospheric dynamical anomaly, component (iv). For the LLCC to generate enough convergence to sustain continuous MCS activity above it, the surface winds almost certainly must be at least 34 knots. A feedback loop between the LLCC's cyclonically curved, convergent inflow feeding the latent heat release, vertical column stretching in the MCS, and lowered surface pressure is then established. This heat engine becomes stronger with the development of a vigorous, anticyclonically curved outflow layer in the upper troposphere, which exports anticyclonic momentum from the system core. For a tropical storm to further organize

into a severe tropical cyclone requires only the development of component (v), which is the formation of the typhoon eye.

The foregoing definitions presume existence of a dynamically and thermodynamically favorable synoptic environment. Without such a dynamical and thermodynamical favorable environment, tropical cyclone formation is not possible. If the environment is dynamically favorable but thermodynamically unfavorable, an organized tropical depression of two anomalous components could persist until it is carried by the environmental winds to a more thermodynamically favorable region where it could further organize. If the environment is thermodynamically favorable, but dynamically unfavorable, tropical cyclone genesis could still take place through vigorous mesoscale convective activity; this is the Ofelia-type case. With both a dynamically and thermodynamically favorable environment, TC formation is possible and even probable. If it occurs predominately through synoptic processes, it would be considered a Robyn-type formation. If MCS activity were also present, it would be called a Combination-type tropical cyclone formation.

V. SUMMARY AND CONCLUSIONS

A. SUMMARY

Severe tropical cyclones annually pose a serious threat to life, property, and military assets around the world. A more complete understanding of their formation processes is necessary to increase the timeliness and accuracy of warnings and reduce the damage. Because the tropical air-ocean environment is often thermodynamically favorable and changes slowly, a study of dynamical variables—including mesoscale convective systems—provides more insight into day-to-day tropical cyclone development processes. Hypotheses that MCSs in a developing tropical disturbance may contribute to a tropical storm formation, and be a factor in determining its future size and intensity, make their detailed observation even more necessary. The lack of timely and reliable conventional or aircraft reconnaissance data in the western North Pacific makes the interpretation of high-resolution geostationary satellite animations critical for observing developing TCs.

Two conceptual models (Harr et al. 1996a, b) formulated during the Tropical Cyclone Motion (TCM-93) mini-field experiment provided the basis for this study of more cases of tropical cyclone formation. The first conceptual model described a tropical disturbance in which the increase in low-level cyclonic vorticity was caused primarily by a centrally located MCS in a thermodynamically favorable environment—this is referred to as the Ofelia-type formation process. The second conceptual model is based on a hypothesis that strong synoptic-scale dynamic forcing (rather than MCS forcing) is the primary mechanism for increasing the low-level relative vorticity of the tropical disturbance—this is the Robyn-type formation.

The primary anlysis tool for these case studies was high-resolution GMS-4 and GMS-5 visible and infrared imagery that was animated for the TC formation period. In addition, NOGAPS fields at 00 and 12 UTC provided an analysis of synoptic-scale phenomena affecting system organization. Potentially significant variables were recorded, including information about the synoptic and mesoscale features in the developing system.

B. RESULTS

The Ofelia-type and Robyn-type conceptual models of tropical cyclone formation were observed (six and two times, respectively) in this sample of 13 case studies. The conceptual models represent separate valid pathways towards tropical cyclone genesis. However, there appear to be situations in which neither conceptual model adequately describes the formation stage because both mesoscale and synoptic-scale processes are observed to operate concurrently to form a tropical cyclone. In all of the Ofelia-type formations, some favorable synoptic-scale dynamic forcing existed even though it was often weak and obviously of secondary importance to the formation. Thus, instead of grouping formations into separate categories, it may be useful to view them as variations on the same theme: the interaction of mesoscale and synoptic-scale processes in a thermodynamically favorable environment.

Analysis of the variables summarized in Tables 3-1 through 3-3 reveals several important characteristics of developing systems. First, tropical cyclones formed primarily by vigorous, sustained MCS activity tend to be smaller than those formed primarily through synoptic-scale processes. This implies that the processes operating during the genesis stage have a lasting impact on the structure—and thus the motion—of the mature

tropical cyclone. Second, MCSs that endure longer than average tend to be associated with systems that are increasing their organization. Third, the redevelopment of a MCS over the tropical system LLCC is a frequent occurrence in developing systems, sometimes occurring days before the transition to tropical storm strength. By contrast, MCSs that form on the periphery may have a small contribution to maintenance of the synoptic system, but do not seem to be associated with TC formation processes. Thus, the MCS location relative to the system LLCC may prove to be a key indicator for separating systems that are likely to increase in organization versus the non-developing systems.

An alternate approach to viewing tropical cyclone formation from satellite imagery may be of operational use. This approach describes the development of a mature tropical cyclone in terms of a grouping of dynamic, thermodynamic and temporal anomalies, each of which is visible in high-resolution satellite animations. A tropical system may then be ranked in level of organization by the number of co-located anomalous components it contains.

Zehr (1992) hypothesized a pathway to tropical cyclone genesis consisting of two stages, each of which is initiated by a surge of wind into the core of a developing tropical disturbance. The wind surges are hypothesized to provide low-level confluence and convergence, which leads to the development of a centrally located MCS. Upon the dissipation of the first MCS, a LLCC is created that is hypothesized to persist from 15 hours to eight days until the next wind surge generates a second, stronger round of convection and the system becomes a tropical storm. Conclusions drawn from the analysis of this data set of 13 tropical cyclone formations differ from the Zehr two-stage model of tropical cyclone development in several respects. First, although numerous

model of tropical cyclone development in several respects. First, although numerous straight-line wind surges were observed, there were no instances of a wind surge penetrating to the center of a developing tropical disturbance. This implies that other dynamical processes must be occurring to initiate centrally located deep convection. Second, in several tropical cyclone formations—notably Typhoons Ellie and Gladys in 1994—more than two convective stages occurred centered over the system LLCC. In some instances of weaker synoptic-scale forcing, more than two cycles of convection are thus required to spin up the low-level vorticity of the system.

C. RECOMMENDATIONS

For future studies of tropical cyclone genesis, the terms "Ofelia-type" and "Robyn-type" formations should be changed to the more general terms "Mesoscale-type" and "Synoptic-type" formations, which better describe the dominant dynamic processes leading to genesis. The use of high-resolution geostationary satellite animation is a valuable tool in studying the formation of tropical cyclones. The implementation of the following items would further increase the utility and add greatly to the understanding of tropical cyclone genesis.

1. Additional case studies. This thesis includes a total of 13 case studies and 61 MCSs culled from nearly 30 tropical cyclone formations. No examples of formations resulting from tropical upper-tropospheric trough (TUTT) cells or over-land MCCs that drifted over the ocean were represented. Additionally, all selected case studies were taken from the western North Pacific basin. This small, potentially basin-biased sample size limits the number and accuracy of the conclusions that may be drawn from the data, especially in regard to meaningful statistical analysis.

2. Non-developing systems. This thesis concentrated exclusively on tropical systems that developed at least to tropical storm intensity. No differences are apparent in the overall amount and intensity of convective cloudiness between developing and non-developing systems (Erickson 1977). Thus, comparisons between developing and non-developing tropical systems would illuminate key factors responsible for the further development of tropical disturbances. This could prove to be valuable to the operational tropical cyclone forecaster to distinguish between systems requiring close monitoring and those that show little sign of further development.

3. A more quantitative analysis. Because of the subjective nature of several variables listed in Tables 3-1 to 3-3, it may prove difficult to maintain continuity from this data set and future case studies analyzed by a different observer. Since both GMS data and NOGAPS analyses are digital, a variety of computer programs can be written to determine the quantitative character of important physical parameters during tropical cyclone genesis. Wind components may be calculated for the synoptic environment—both zonal, as in Figs. 5.C.1 and 5.C.2, and meridional—and cyclonic vorticity values may be determined. This provides a more quantitative means of characterizing the synoptic environment rather than the use of categories such as "monsoon depression," "equatorial wave," and the like.

Coded with pre-defined conditions for separating MCSs from non-MCS tropical convection—as in Chapter IB—a computer program can be written to locate objectively and track all MCS developments within a specified geographic region. From multiple analyses, MCS size and duration distributions may be derived and compared for mesoscale- and synoptic-type formations, as in Fig. 5.C.3 and Fig. 5.C.4. A large

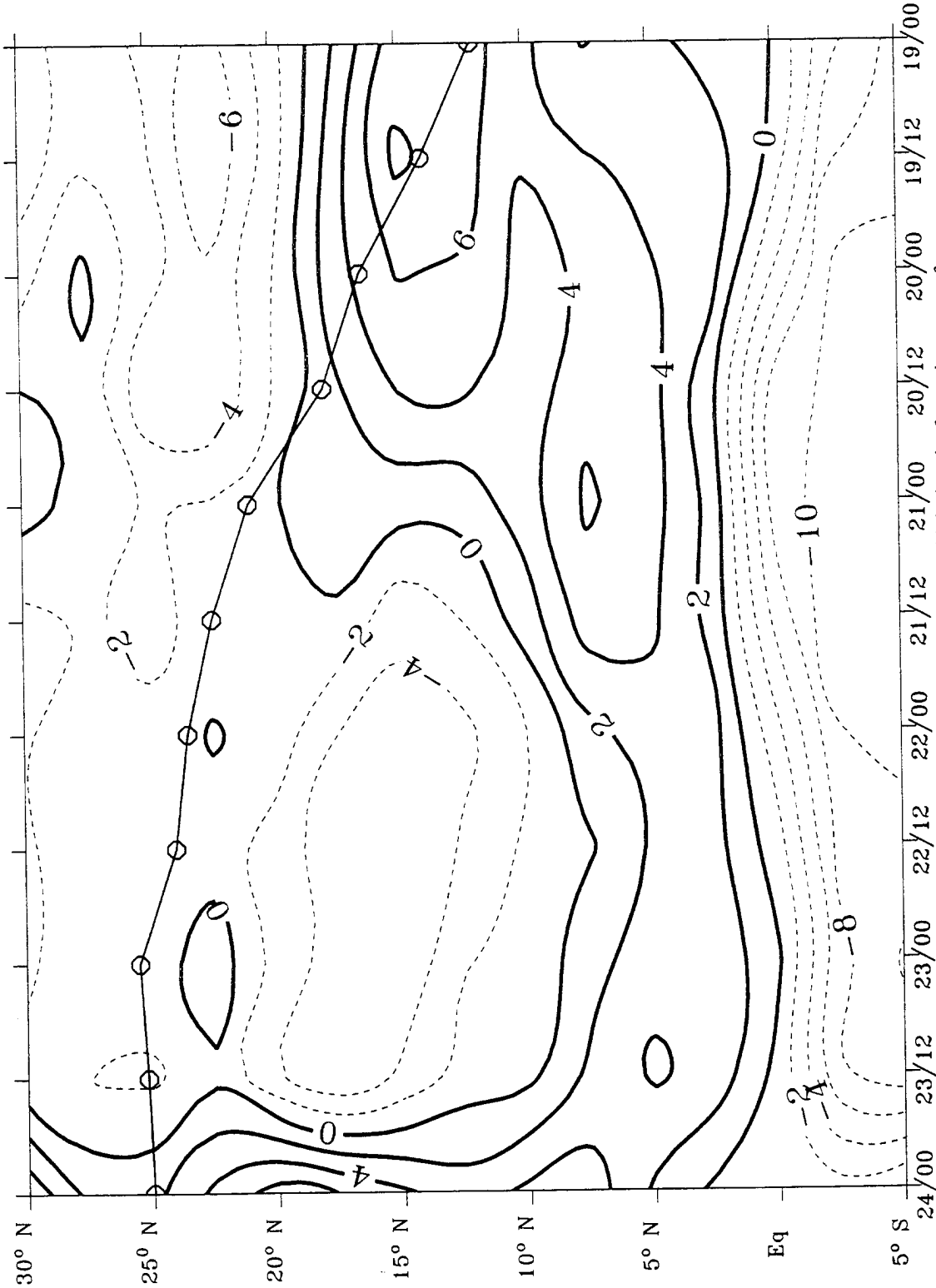

Fig. 5.C.1 Latitude—time plot of NOGAPS 850 mb zonal wind field during the formation stage of Typhoon Gladys, 19-24 August 1994. Latitude increases along the X axis and time increases left along the Y axis. Solid lines indicate westerlies, dashed lines indicate easterlies, and circles indicate the 12 hourly JTWC best-track position of the tropical system center.

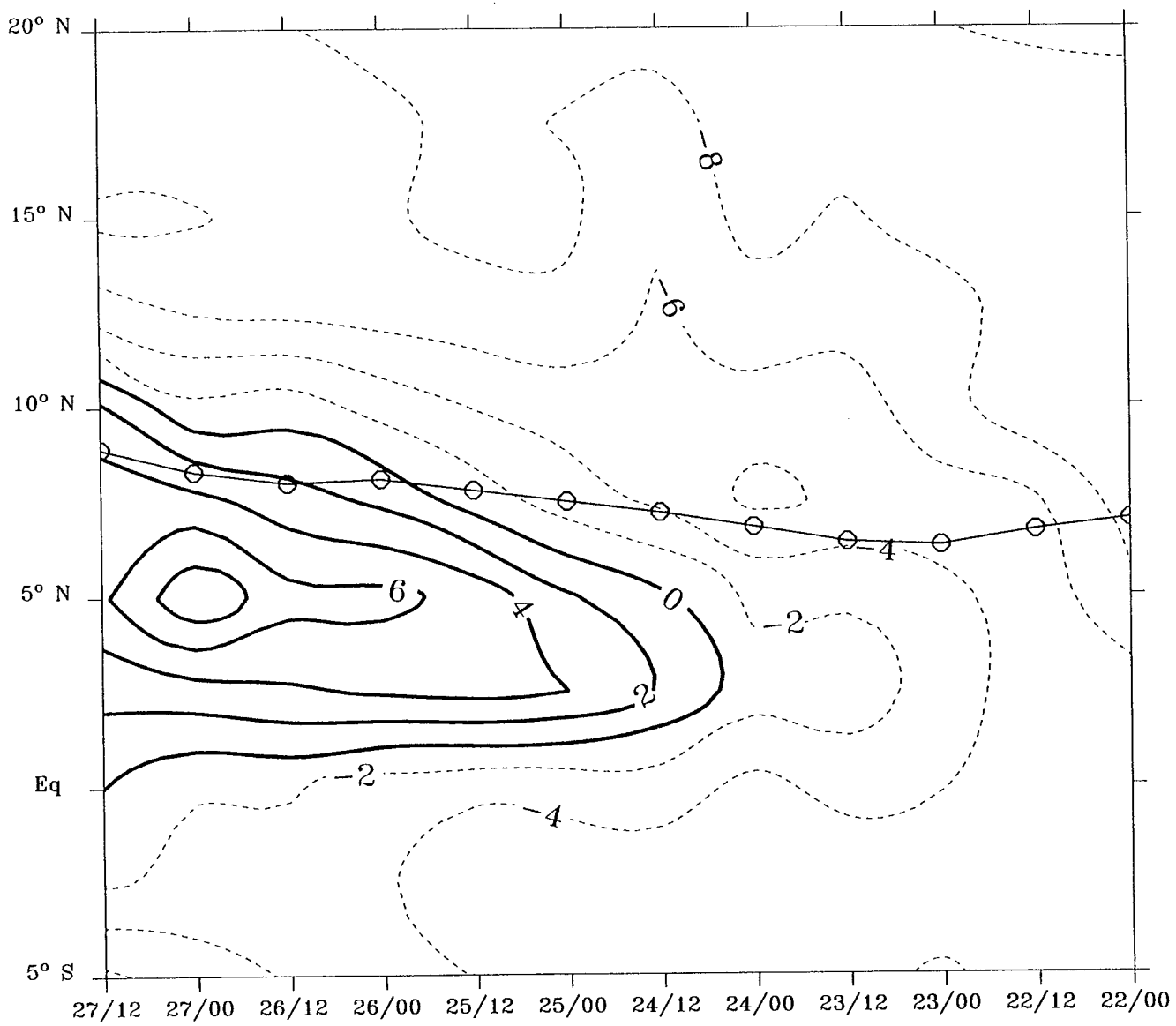

Fig. 5.C.2 As in Fig. 5.C.1, except for the formation stage of Typhoon Sibyl from 22-27 July 1995.

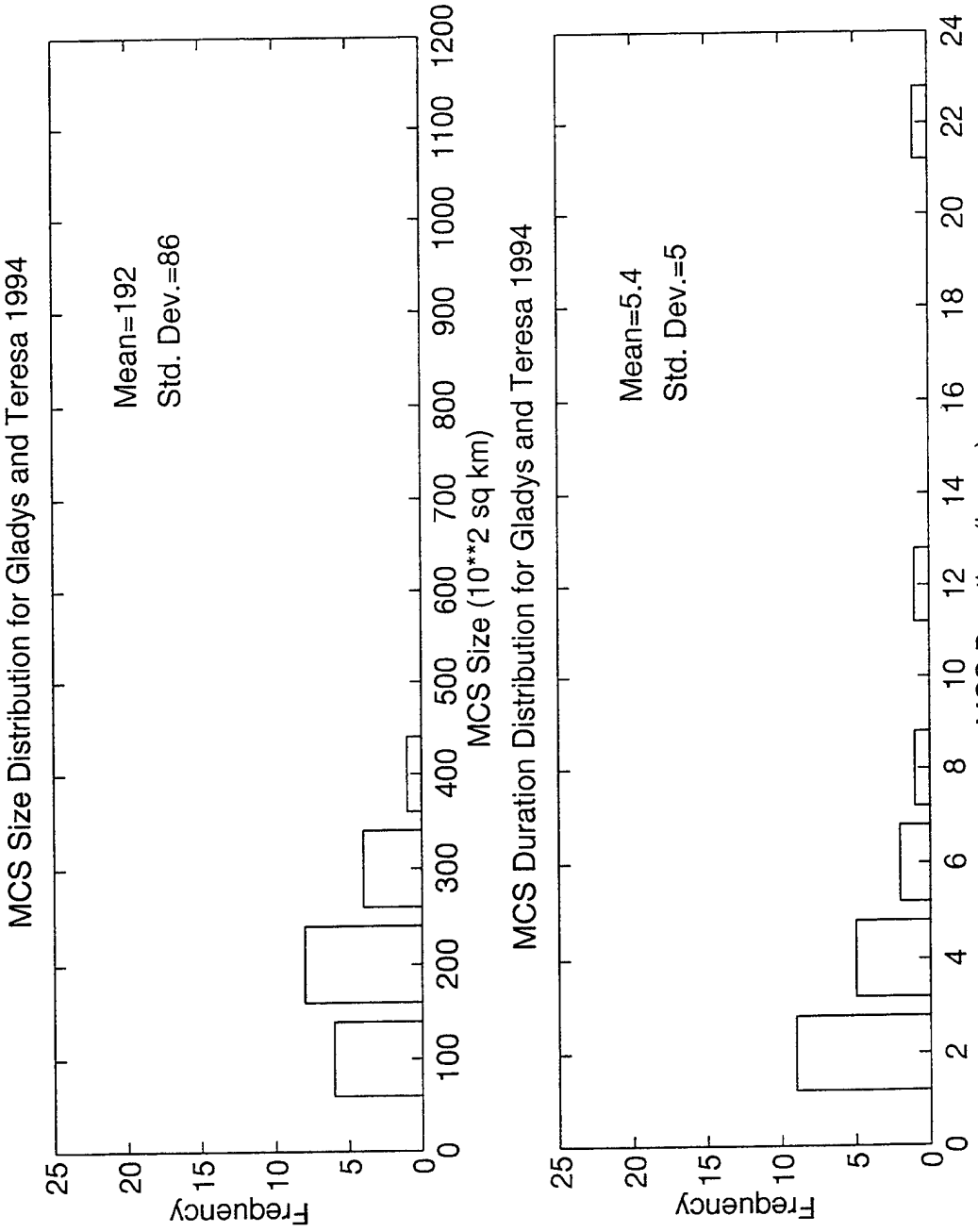

Fig. 5.C.3 MCS size and duration distributions for Typhoons Gladys and Teresa, 1994.

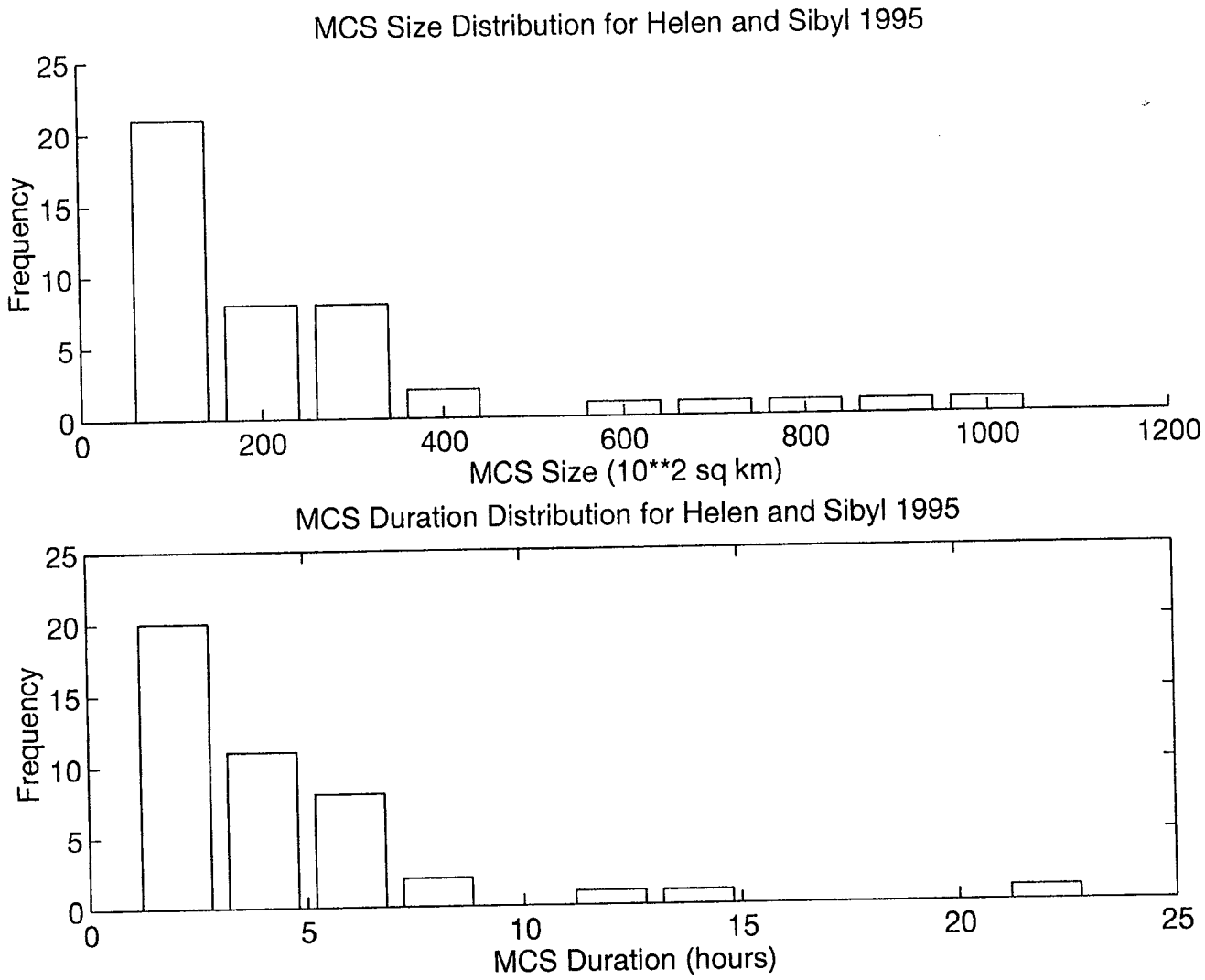

Fig. 5.C.4 As in Fig. 5.C.3, except for Typhoons Helen and Sibyl, 1995.

database of such objective analyses may provide insight into the structural differences between typical MCSs in different formation types.

Using the post-storm best-track positions from the JTWC Annual Tropical Cyclone Report, system center-relative locations of all MCSs and their movement may be tracked. Statistical analysis of a larger sample may reveal differences in MCS location and movement patterns of different formation types, as suggested by Fig. 5.C.5 and Fig. 5.C.6. They indicate that for mesoscale-type formations (Fig. 5.C.5) the majority of MCSs occur near the system center and are potentially important to the overall system development. For synoptic-type formations (Fig. 5.C.6), MCSs appear to be distributed over a greater area with a greater tendency to rotate relative to the system center.

Another objective, center-relative analysis technique divides the tropical disturbance area by azimuth and distance from the JTWC best-track center (Fig. 5.C.7). By depicting GMS infrared satellite imagery for specified brightness temperature ranges over a one- to two-degree latitude annulus, a timeline display is generated showing the growth, development, movement, and dissipation of deep convection throughout the developing system (Fig. 5.C.8 and Fig. 5.C.9). Patterns not easily observed in other displays are revealed through these time-azimuth diagrams. Using one or several of these proposed quantified approaches of analyzing MCS activity, the inevitable variability introduced by a human analyst will be reduced and yield better statistical analyses.

4. GMS-5 capabilities. The GMS-5 satellite has several capabilities not found on the GMS-4 that can be used to further improve the analysis of developing tropical cyclones. A new infrared channel designed for detection of atmospheric water vapor will provide more information about the horizontal and vertical motion in and around the

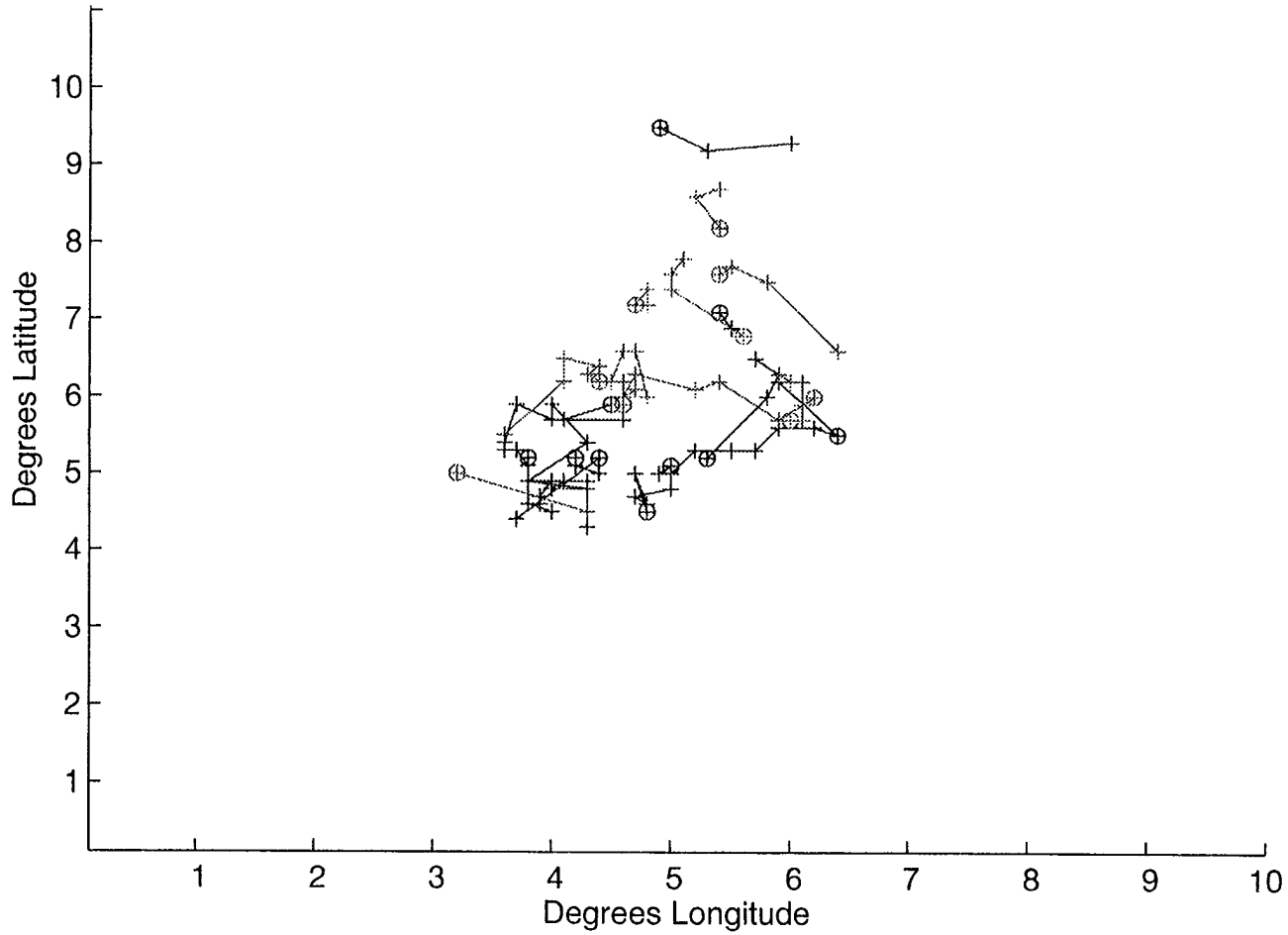

Fig. 5.C.5 System center-relative tracks of convective cloud clusters for Typhoons Gladys (solid lines) and Teresa (dotted lines), 1994. The lines are separated in one hour increments and circles indicate formation location. System centers are located at five degrees latitude and five degrees longitude.

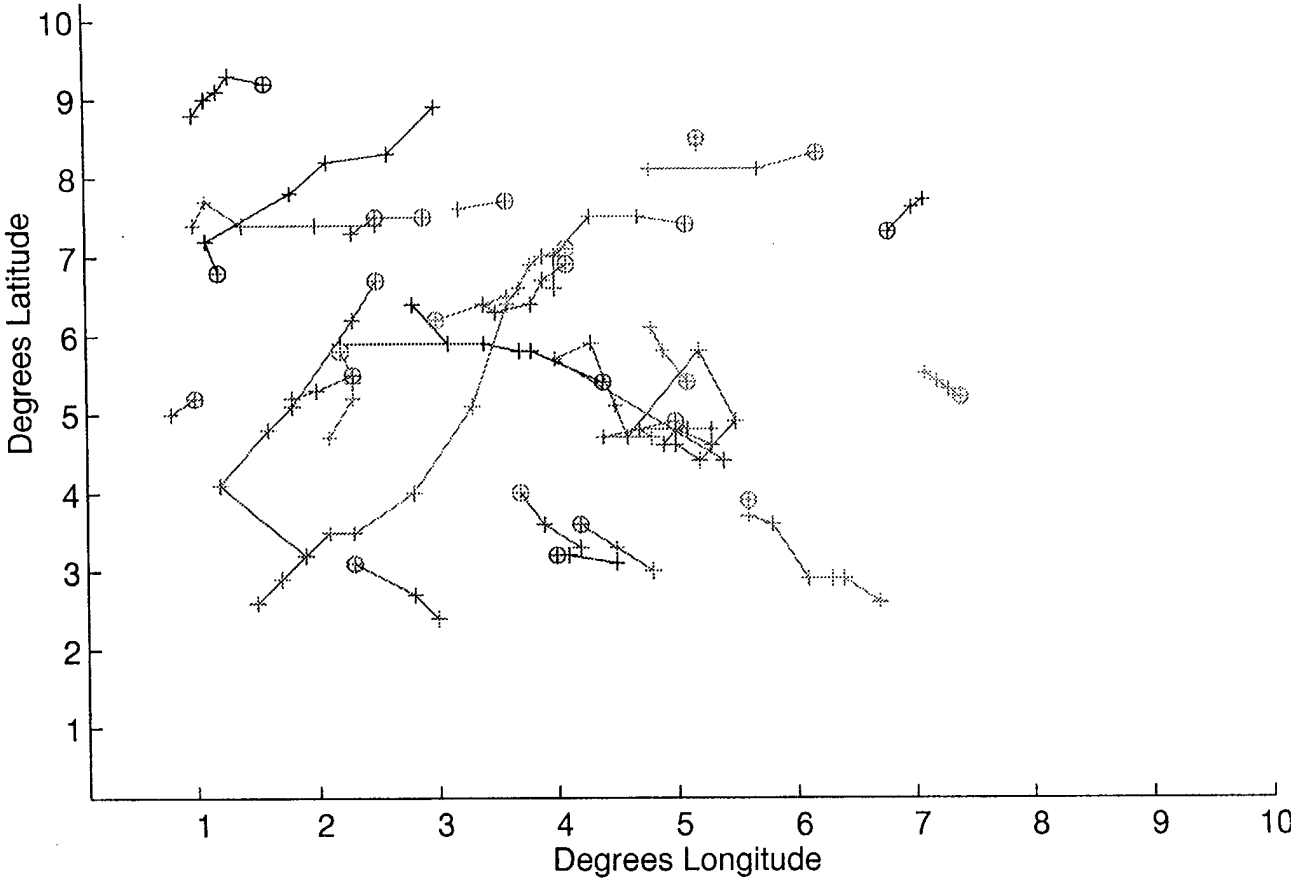

Fig. 5.C.6 As in Fig. 5.C.5, except for Typhoon Sibyl, 1995. Pre-organization stage convective cloud clusters are indicated by solid lines, organization stage convective cloud clusters are indicated by dotted lines.

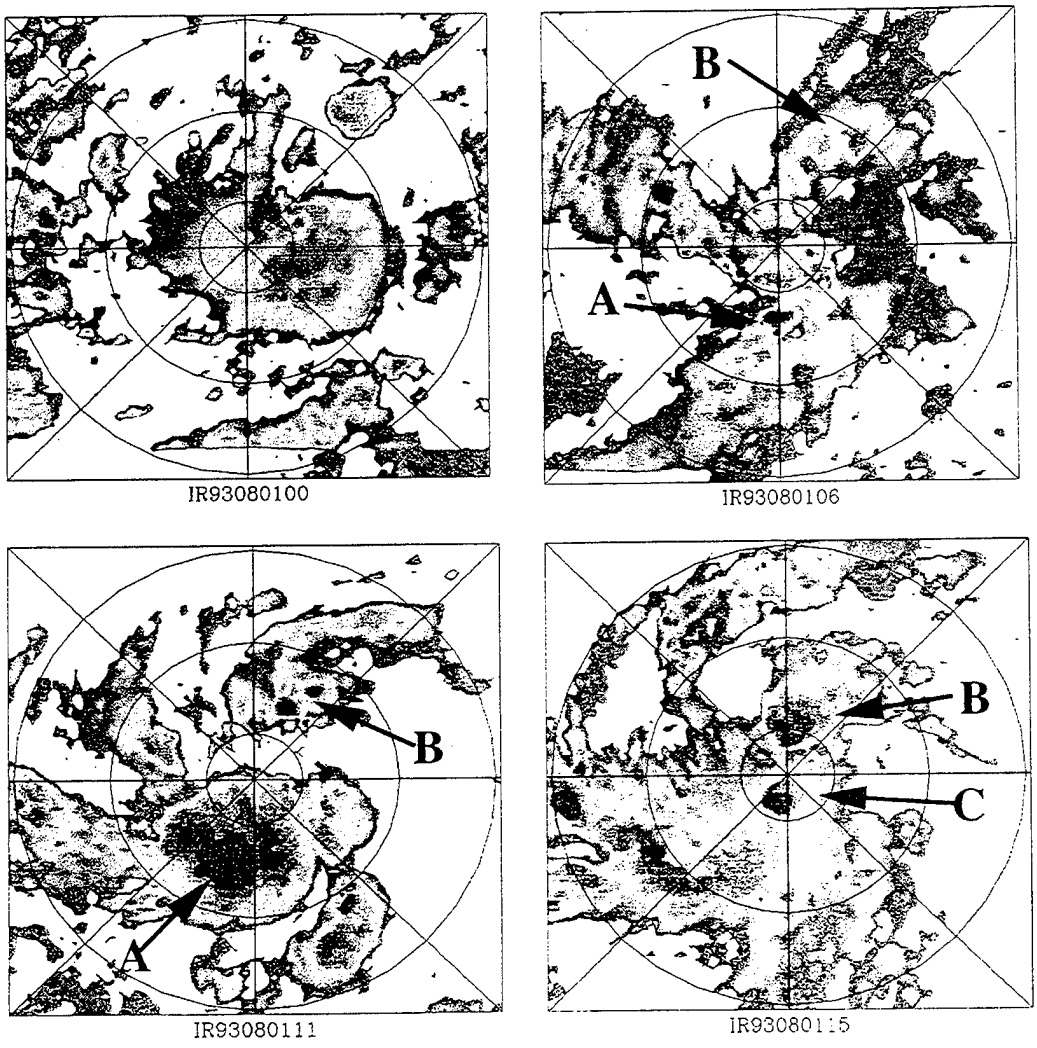

Fig. 5.C.7 Infrared GMS images centered on JTWC best-track position during formation stage of Typhoon Robyn, 1993. Arrows indicate development and movement of MCSs A, B, and C during a 15-hour period.

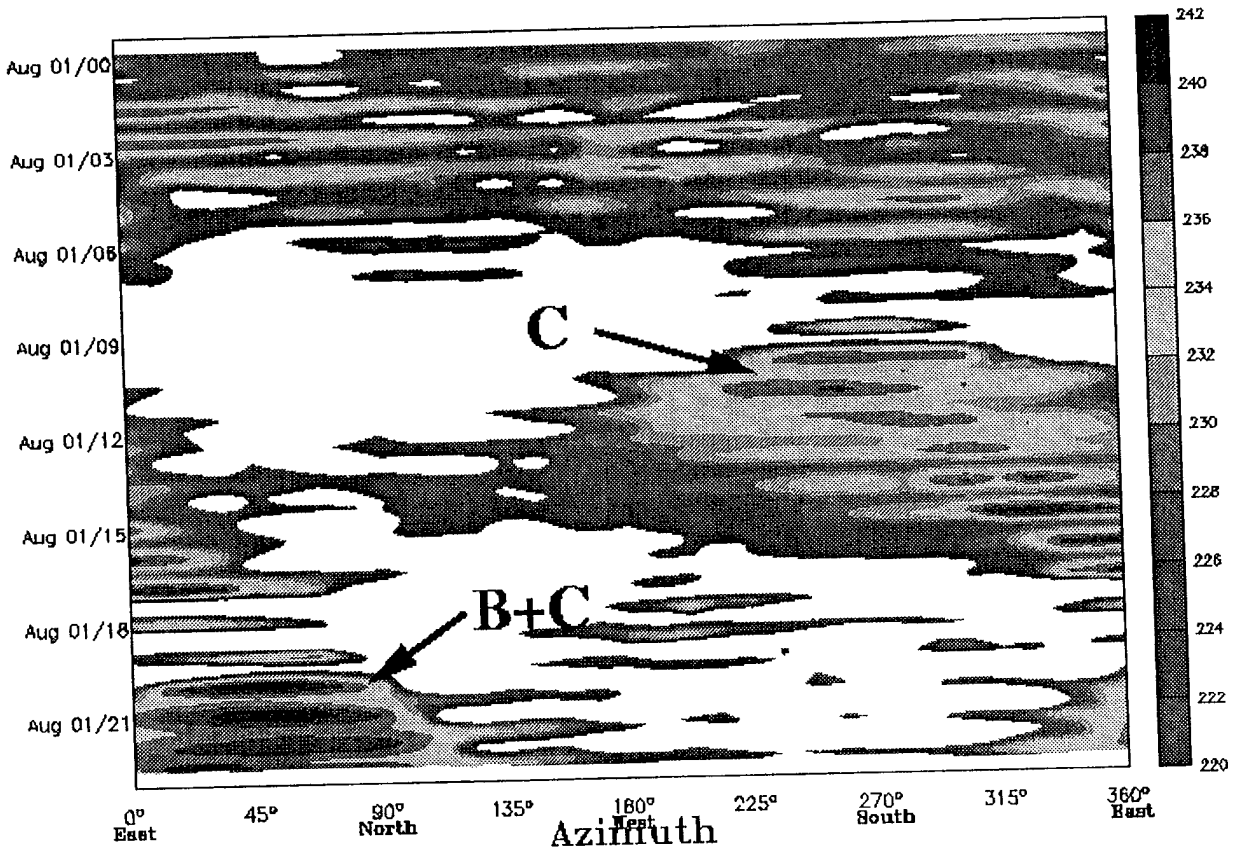

Fig. 5.C.8 Time—azimuth display of GMS digital infrared values (scale shown on right side) related to cloud-top temperatures in an annulus from zero to one degrees radius from the JTWC best-track system center during the formation stage of Typhoon Robyn, 1993. Values less than 220 are white and represent warmer cloud top temperatures not associated with deep tropical convection.

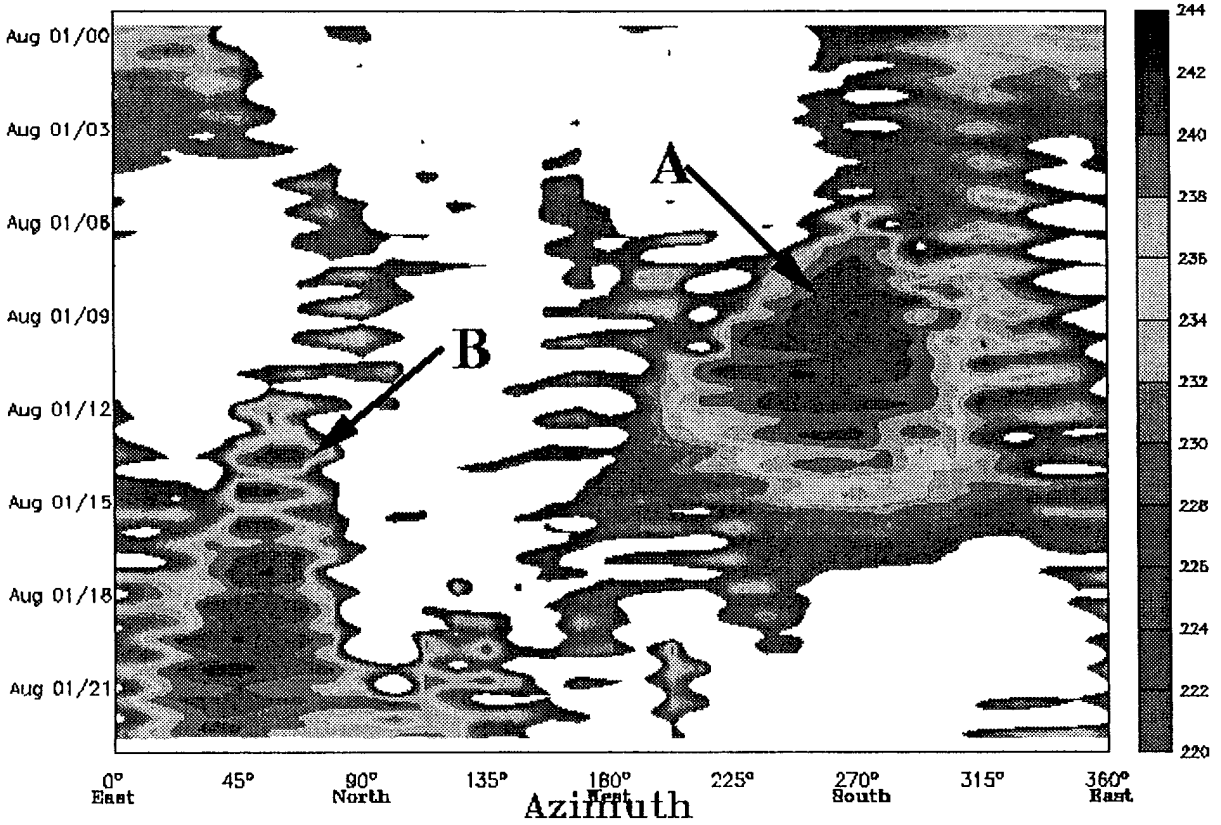

Fig. 5.C.9 As in Fig. 5.C.8, except for one to three degrees radius from the JTWC best-track system center.

tropical disturbance. The introduction of automated water vapor and cloud-drift wind analyses will greatly improve the detection of a developing upper-level outflow region and may simplify the process of determining the tropical system low-level outer wind profile.

REFERENCES

Chen, L. S., 1995: Tropical cyclone heavy rainfall and damaging winds. Chap. 6, Tech. Doc. No. 693, *Global Perspectives on Tropical Cyclones* (R. L. Elsberry, ed.), World Meteor. Organiz, Geneva, Switzerland, 261-289.

Chen, L. S., and Frank, W. M., 1993. A numerical study of the genesis of extra-tropical convective meso-vortices. Part I: Evolution and dynamics. *J. Atmos. Sci.,* 50, 2401-2426.

Elsberry, R. L., G. Foley, H. Willoughby, J. McBride, I. Ginis, and L. Chen, 1995: *Global Perspectives on Tropical Cyclones.* Tech. Doc. No. 693, World Meteor. Organiz, Geneva, Switzerland, 289 pp.

Erickson, S. L., 1977: Comparison of developing and non-developing tropical disturbances. Paper No. 274, Dept. of Atmos. Sci., Colo. State Univ., Ft Collins, CO 80523, 81 pp.

Gray, W. M., 1975: Tropical cyclone genesis. Paper No. 323, Dept. of Atmos. Sci., Colo. State Univ., Ft. Collins, CO 80523, 121 pp.

Gray, W. M., 1979: Hurricanes: Their formation, structure and likely role in the tropical circulation. *Meteorology over the Tropical Oceans*, D. B. Shaw (Ed.), Roy. Meteor. Soc., James Glaisher House, Grenville Place, Bracknell, Berkshire, UK, 155-218.

Harr, P. A., M. S. Kalafsky, and R. L. Elsberry, 1996a: Environmental conditions prior to formation of a midget tropical cyclone during TCM-93. *Monthly Weather Review*, 124, 634-652.

Harr, P. A, R. L. Elsberry, and J. C.-L. Chan, 1996b: Transformation of a large monsoon depression to a tropical storm during TCM-93. *Monthly Weather Review*, 2625-2643.

McBride, J. L., 1995: Tropical cyclone formation. Chap. 3, Tech. Doc. No. 693, *Global Perspectives on Tropical Cyclones* (R. L. Elsberry, ed.), World Meteor. Organiz, Geneva, Switzerland, 63-105.

Nuss, W. A., and D. W. Titley, 1994: Use of multiquadric interpolation for meteorological objective analysis. *Monthly Weather Review*, 122, 1611-1631.

Riehl, H., 1954: *Tropical Meteorology*. McGraw-Hill, New York, 392 pp.

Velasco, I., and J. M. Fritsch, 1987: Mesoscale convective complexes in the Americas. *J. Geophys. Res.*, 92, 9591-9613.

Zehr, R. M., 1992: Tropical cyclogenesis in the western North Pacific. Tech. Rep. 61 NESDIS, NOAA, Washington D.C., 20233, 181 pp.

INITIAL DISTRIBUTION LIST

		No. Copies
1.	Defense Technical Information Center 8725 John J. Kingman Road., Ste 0944 Ft. Belvoir VA 22060-6218	2
2.	Dudley Knox Library Naval Postgraduate School 411 Dyer Rd. Monterey CA 93943-5101	2
3.	Meteorology Department Code MR/Wx Naval Postgraduate School 589 Dyer Rd Rm 252 Monterey CA 93943-5114	1
4.	Dr. R. L. Elsberry Code MR/Es Naval Postgraduate School 589 Dyer Rd Rm 252 Monterey CA 93943-5114	2
5.	Dr. P. A. Harr Code MR/Hr Naval Postgraduate School 589 Dyer Rd Rm 252 Monterey CA 93943-5114	2
6.	Dr. E. Ritchie Code MR/Ri Naval Postgraduate School 589 Dyer Rd Rm 252 Monterey CA 93943-5114	1
7.	Capt Christopher A. Finta 36 OSS/OSJ PSC 489, Box 20 FPO AP 96536-0051	1

8. Chief of Naval Research 1
800 N Quincy Street
Arlington VA 22217

9. Commanding Officer 1
Naval Pacific Meteorology and Oceanography Center
COMNAVMARIANAS Box 12
FPO AP 96540-0051

10. Dr. Mark Lander 1
c/o: 36 OSS/OSJ
PSC 489, Box 20
FPO AP 96536-0051

11. Superintendent, Naval Research Laboratory . . . 1
7 Grace Hopper Ave Stop 2
Monterey CA 93943-5502